RE-EVALUATION OF EXISTING FATIGUE CODES IN EUROCODE 3.1-9

A DISSERTATION

Submitted in partial fulfillment of the requirements for the award of the degree

Of

MASTERS OF TECHNOLOGY

In

METALLURGICAL AND MATERIALS ENGINEERING

(with specialization in Materials Engineering)

By

PRIYANKA ARORA

METALLURGICAL AND MATERIALS ENGINEERING DEPARTMENT

INDIAN INSTITUTE OF TECHNOLOGY ROORKEE

ROORKEE-247667 (INDIA)

MAY 2018

CANDIDATE'S DECLARATION

I hereby declare that the work presented in the dissertation entitled "**RE-EVALUATION OF EXISTING FATIGUE CODES IN EUROCODE 3.1-9"** is submitted in partial fulfillment of the requirements for the award of the degree of Master of Technology with specialization in Materials Engineering, to the Department of Metallurgical & Materials Engineering, Indian Institute of Technology Roorkee and is an authentic record of my own work carried out under the guidance and supervision of Prof. P. K. Ghosh and Dr. Vivek Pancholi, Department of Metallurgical & Materials Engineering, Indian Institute of Technology, Roorkee and Prof. Dr.-Ing. Thomas Ummenhofer and Prof. Dr.-Ing. Peter Knoedel, Karlsruhe Institute of Technology, Karlsruhe, Germany. I have not submitted the matter embodied in this report for the award of any other degree or diploma.

Date:

Place: Roorkee (Priyanka Arora)

CERTIFICATION

This is to certify that the above statement made by the candidate is correct to the best of my knowledge and belief.

Dr. Vivek Pancholi,
Associate Professor,
Department of Metallurgical & Materials Engineering,
Indian Institute of Technology Roorkee.

ABSTRACT

Steel structures are being built worldwide for more than 120 years. The effects of repetitive loading i.e. fatigue on steel structures such as bridges or towers have been extensively studied since the 1960s. The work and lessons learned from the poor performance of some structures have led to the better understanding of fatigue behavior. In 1985, consequent appearances of the first European Convention for Constructional Steelwork (ECCS) recommendations on fatigue design have changed the spirit radically. At European level, the ECCS recommendations contains first unified fatigue rules, followed by the development of structural Eurocodes.

Eurocode 3 defines values of fatigue strength for particular structure on the basis of which designing of the structure is being carried out since last 58 years. However, many factors have improved over these years like quality and consistency of material and its properties, improvement in welding techniques, and reliable testing data. So an important initiative is undertaken by research community in Europe to redefine the pre-existing fatigue values. The initiative is based on the fact that the earlier analysis was done considering a high factor of safety or with low confidence limit. In view of this present work was planned to study the" Existing Fatigue Codes in Eurocode 3.1-9"and its Re-Evaluation by applying statistical approach on the available data.

Efforts were made to collect existing fatigue data on Eurocode 3.1-9 Fatigue Classes. The background document available in this regard was thoroughly analyzed in order to find out the efficacy of the existing fatigue classes in Eurocode 3.1-9. In the process of such analytical activities, the existing data will be appropriately classified for their best relevance to applications. Statistical approach has been applied on the collected data to know the value of fatigue by doing the analysis for 95% survival probability at 2 million cycles by making use of prediction interval. Also, the addition of two more codes in EC 3.1-9 has been recommended after doing the study on one more code given by International Institute of Welding (IIW) named as "Recommendations for fatigue design of welded joints and components".

ACKNOWLEDGEMENT

I would like to express my deep sense of gratitude and sincere thanks to my beloved guide **Dr. Vivek Pancholi**, Department of Metallurgical & Materials Engineering, Indian Institute of Technology Roorkee, for being so supportive, patient and great source of inspiration. I would like to thank my supervisor **Prof. Dr.- Ing. Peter Knoedel and Dipl. Ing. Benjamin Seyfried** and Head of Civil Engineering Department, **Prof. Dr.- Ing. Thomas Ummenhofer**, Karlsruhe Institute of Technology, karlsruhe, Germany for their keen interest and constant encouragement which gave me confidence to complete my work. Despite their busy schedule, I was given valuable suggestions. Their dedication to work and self-belief will always inspire me, and I hope to continue to work with their noble thoughts.

I would like to take this time to thank other faculty members of the department for their valuable suggestions and motivation.

I would like to extend my gratitude to my friends and classmates for their support throughout the past two years. I owe a lot to my family who unremittingly supported me during my years of study. I would like to pay high regards to my parents for being a true motivator throughout my life. Their relentless backing made this work possible and I would like to dedicate it to them.

Priyanka Arora

TABLE OF CONTENTS

LIST OF FIGURES

LIST OF TABLES

Chapter 1 INTRODUCTION

In 1975, the Commission of the European Community adopted an action program in the field of construction, based on Article 95 of the Treaty. The objective of the program was to remove technical barriers to trade and to harmonize technical specifications. In the framework of this action program, the Commission took the initiative to establish harmonized technical rules for the design of structures, which in a first phase would serve as an alternative to the national rules in force in the Member States and ultimately replace them. For 15 years, with the help of a Steering Committee with Member State representatives, the Commission carried out the development of the Eurocodes program, which led to the first generation of European codes in the 1980s.

In 1989, the Commission and the Member States of the EU and EFTA decided, on the basis of an agreement between the Commission and CEN in order to transmit to CEN the preparation and publication of Eurocodes through a series of mandates to give them a future status of the European Standard (EN).

The Structural Eurocodes programme comprises the following standards generally consisting of a number of parts:

EN 1990	Eurocode 0:	Basis of Structural Design
EN 1991	Eurocode 1:	Actions on Structures
EN 1992	Eurocode 2:	Design of Concrete Structures
EN 1993	Eurocode 3:	Design of Steel Structures
EN 1994	Eurocode 4:	Design of Composite Steel and Concrete structures
EN 1995	Eurocode 5:	Design of Timber structures
EN 1996	Eurocode 6:	Design of Masonry Structures
EN 1997	Eurocode 7:	Geotechnical design

EN 1998 Eurocode 8: Design of structures for Earthquake resistance

EN 1999 Eurocode 9: Design of aluminum Structures

The Eurocodes standards recognize the responsibility of the regulatory authorities in each Member State and have protected their right to set values on issues of regulatory certainty at national level, where these vary from state to state [1].

Eurocode 1993 part 1-9 provides methods for evaluating the fatigue strength of components, joints and joints subject to fatigue loading. These techniques are derived from fatigue tests on large-area samples that include geometric and structural imperfections from material fabrication and design, such as the effects of tolerances and residual stress in welding. The rules apply to structures in which the design complies with EN 1090 and also specifies the corresponding and supplementary requirements in the detailed category tables. The valuation methods i.e. the damage tolerance method and the safe life method are applicable to all grades of structural steels, stainless steels and unprotected reinforcing bars, unless otherwise specified in the detailed category tables. This part only applies to materials meeting the strength requirements of Eurocode 3.1-10. Other fatigue assessment methods than stress reduction are not covered in this section. Post-treatment that are done to improve fatigue resistance other than stress relief are not included in this section. The fatigue strengths method given applies only to the structures operating under normal atmospheric conditions, regularly maintained with adequate corrosion protection. The effect of corrosion caused due to sea water is not been covered. Microstructure damage caused by high temperatures (> 150°C) is also not covered [1].

Fatigue is defined as material weakening caused by exposure to repeated loading. It is a progressive and local structural damage that occurs when a material is subjected to cyclic loading. The nominal maximum stress values that can cause such damage are much less than the yield stress or ultimate tensile yield stress of the material. If the loads or stresses applied are above a certain threshold then the microscopic cracks are formed on the stress concentrators such as the persistent slip bands, surface, grain interfaces in the case of metals and component interfaces in the case of composites. Eventually when a crack reaches a certain critical size, the crack propagates at a faster rate and the structure will ruptures resulting in failure. The shape of the structure or geometry significantly affects the fatigue life. Square holes or sharp corners results in an increase in the local stresses making that region more prone to fatigue failure. Round holes and smooth transitions or fillets therefore increase the fatigue strength of the structure [2].

Fatigue failure occurs in four different stages:

1. Crack nucleation,
2. Crack-growth 1st stage,
3. Crack-growth 2nd stage, and
4. Ultimate failure.

Chapter 2 LITERATURE REVIEW

2.1 Design of steel structure on the basis of fatigue

According to the terminology used in EN 1993-1-9 (TGC 10, 2006), fatigue can occur when a component is subjected to repeated cyclic loading due to the effects of stress fluctuations [3]. As already discussed, the fatigue phenomenon manifests itself as cracks that develop at certain points in the structure. These cracks can occur in various types of structures such as aircraft, bridges, boats, frames (of cars, locomotives or wagons), overhead cranes, cranes, machine parts, turbines, reactor ships, locks doors, offshore platforms, transmission towers, pylons, masts and chimneys. In general, structures exposed to repeated cyclic loads may be subjected to progressive damage and this has been evidenced by crack propagation. This damage to the structure is termed as fatigue and is represented as loss of resistance/strength with time. Fatigue fractures rarely occur in the base material, away from any design details, machining details, welds, or joints. Even if the static resistance of the connection is superior to that of the assembled elements, the connection and the joints always remains the critical point from the standpoint of fatigue.

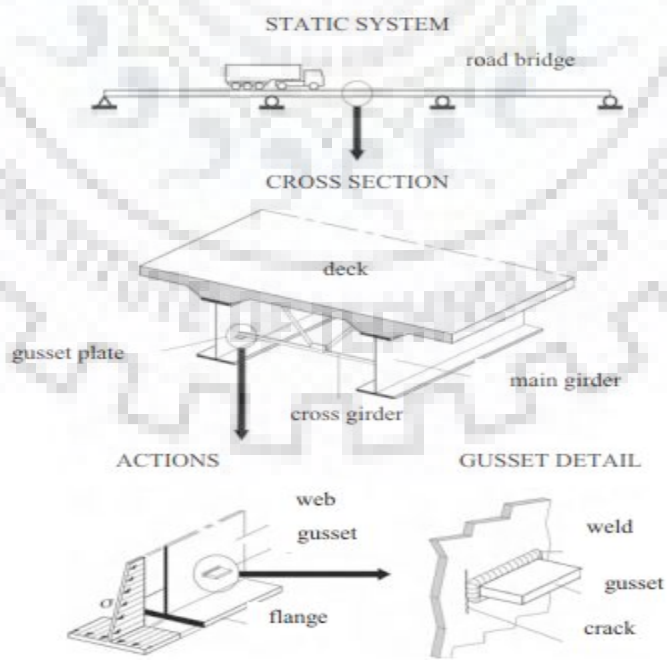

Figure 1. Location possible for fatigue crack in a steel & composite road bridge

Fig. 1 schematically shows the traffic-loaded steel and concrete composite road bridge. Every vehicle crossing the bridge leads to cyclic loadings and thus causing stresses in the structure. The induced stresses are due to the presence of the attachments such as those who connects the cross member/girders to the main carriers/girders influenced. At the ends of the fasteners, mainly at the weld toes, connecting them to the remainder of the structure, stress concentrations mainly occurs due to the change in the geometry of the structure, due to the presence of the attachments. The same places also show discontinuities those results due to welding. In the field of fatigue, numerous studies were carried out; Wohler in 1860 started his study on rail axes around 150 years ago [4]. The studies showed that the combined effect of stress concentrations and discontinuities can be the source of fatigue crack formation and propagation; even if the applied stresses is below than the material yield stress (applied stresses are the calculated stresses with elastic structural analysis, taking into account the possible residual stresses and stress concentrations). A crack generally develops from discontinuities with a depth of the order of a few tenths of a millimeter. The propagation of crack results in failure of the net section resulting in brittle fracture, which mainly depends on the materials properties, element geometry, and temperature and stress strain rate of the net section. Therefore, a structure subjected to repeated cyclic loads must be carefully designed and fabricated to avoid fatigue failure. Quality assurance methods must ensure that the number and dimensions of existing discontinuities are within tolerance limits.

2.2 Parameters influencing fatigue life

The fatigue life of a member subjected to repeated cyclic loadings is termed as the number of stress cycles it can stand before failure. Depending upon the member or structural detail geometry, its fabrication or the material used, four main parameters can influence the fatigue strength are:

1. Stress difference or stress range
2. Structural geometry detail
3. Materials characteristics
4. Environmental Conditions.

2.2.1 Stress range

Fig. 2 shows the evolution of stress as a function of the time t varying between σ_{min} and σ_{max} for a constant amplitude loading. The fatigue tests have shown that the stress range $\Delta\sigma$ is the main parameter that influences the fatigue life of welded structures or details. The stress range is defined by equation below:

$\Delta \sigma = \sigma_{max} - \sigma_{min}$ 1

Where,

σ_{max} = maximum value of stress (with sign)

σ_{min} = minimum value of stress (with sign)

Other parameters such as min. stress σ_{min}, max. stress σ_{max}, their mean stress σ_m or their ratio known as stress ratio R and the cycle frequency ie number of cycles to failure can be neglected for designing purpose for welded details or structures.

$\sigma_m = (\sigma_{max} + \sigma_{min})/2$.. 2

$R = \sigma_{min} / \sigma_{max}$ 3

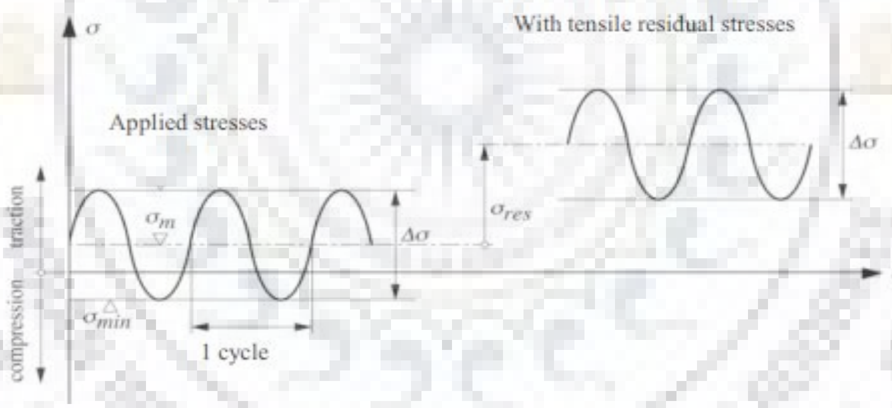

Figure 2 Influence of tensile residual stresses with respect to applied stresses [5]

The fatigue life of a structure can be increased if the stress cycles are partly compressive, but this is not true for welded structures, because of the residual stresses induced in the structure due to welding. The behavior of a crack is influenced by the combined effect of the applied and the residual stresses (Fig. 2). In certain cases, however, a longer fatigue life can be obtained by introducing residual compressive stresses by performing some applications of weld improvement techniques or by doing post treatments after welding.

2.2.2 Structural geometry detail

The geometry of the structural detail is critical to the location of the fatigue crack and its rate of propagation and hence it directly affects the fatigue life of the structure or detail. The elements shown in Figure 3 allow the representation of the three categories of geometric influences:

- Effect of the geometry of the structure, e.g. Sharp edges, the type of cross-section,
- Effect of stress concentration caused by the attachments,
- Effect of discontinuities and cracks in the welds.

The effects of the structure geometry and the stress concentrations can be favorably influenced by a good design of the structural details. A good design is indeed of the utmost importance, as sharp geometric changes (for example due to attachment) affect the flow of stress. This is similar to the velocity of water in a river that is affected by the width of the riverbed or obstacles. In an analogous manner, stresses at the weld of a fixture are higher than the applied stresses. This explains why stress concentrations are created by attachments such as gussets, screw holes, welds or simply by a section change. The influence of discontinuities in the welds can be avoided by means of suitable manufacturing and control methods to ensure that these discontinuities do not exceed the limits of the corresponding quality class according to EN 1090-2. [6] In addition, it must be made clear that discontinuities in the welds can be caused by the welding process (cracks, binding events, lack of fusion or penetration, undercuts, porosity, etc.) and rolling, or grinding, or even corrosion pits. Depending on their shape and dimension, these discontinuities can drastically reduce the fatigue life expectancy of a welded element. The fatigue life can be further reduced if the bad detail is in a stress concentration zone.

2.2.3 Materials characteristics

During fatigue tests on plain metallic specimens or non-welded specimens made up of steel or aluminum alloys, it has been observed that the mechanical properties, chemical composition and microstructure of the metal play a significant role on fatigue life. Thus, a metal with higher tensile strength may have a longer fatigue life under the same stress range, because of an increase in the crack initiation rate rather than an increase in the crack propagation phase. Unfortunately, this positive influence of fatigue because of materials strength is not valid for welded components and structures, as the fatigue life for welded components is mainly determined by the crack propagation phase. Hence in fatigue design for welded structures, the tensile strength of the material does not have any influence. But there are few exceptions to this rule especially for milled and post-treated compounds [5].

2.2.4 Influence of environment on fatigue

A corrosive (water, air, acids, etc.) or humid environment can drastically reduce the fatigue life of metallic elements due to an increase in the crack propagation rate, especially in case of aluminum elements. Therefore, specific corrosion protection such as cathodic protection or special painting systems is required for those encountered on offshore platforms or in the vicinity of chemical plants. On the other hand, with weather-resistant steels used in construction, the superficial corrosion that usually occurs in the weldments has virtually no effect on the fatigue life. In fact the small corrosion pits responsible for possible fatigue cracking are not much critical than the discontinuities which are normally introduced due to welding. In the normal temperature range, the influence of temperature on fatigue crack propagation can be neglected but in case of high temperature application, temperature effects should be considered such as in gas turbines or aircraft engines. However, a low temperature can significantly reduce the critical crack size.

The size of the crack in failure does not significantly affect the material fatigue properties causing premature brittle fracture of the element [7]. Finally, in nuclear power plants where stainless steels are used, neutron irradiation leads to steel embrittlement [8], making them more susceptible to brittle fracture and also reducing their fatigue resistance properties.

2.3 Determination of expression for fatigue strength

To know the fatigue strength of a given structure, it is required to carry out an experimental investigation during which test specimens are subjected to repeated cyclic loading so that a sinusoidal stress range is formed as shown in Fig. 3. The test specimen should be big enough so that it properly represents the structural detail. The number of test specimens should be large enough so that the scattering of the results are properly measured. Even under similar testing conditions the number of cycles to failure may not be same for apparently identical test specimens. This is because of small differences in the parameters which may influence fatigue life (tolerances, misalignments, discontinuities, etc.). The test results of welded specimens are usually drawn on a S-N curve with the number of cycles N to failure on the abscissa and with the stress range $\Delta\sigma$ on the ordinate as shown in Fig. 3.

The fact is that the scatter of the test results is less at high ranges and larger at low stress ranges [7] [8].

By using the logarithmic scale for both the axes, the mean value of the test results for a given structural detail can be expressed by a straight line in the range between 10^4 cycles and $5.\ 10^6$ to 10^7 cycles, by following expression:

$N = a.\ (\Delta\ \sigma)^{-\ m}$ …………..……………………………………………..4

Where,

N= number of cycles for stress range $\Delta\ \sigma$,

a = constant representing the influence of the structural detail,

$\Delta\sigma$ = stress range for constant amplitude,

m = slope coefficient of mean regression line.

The above expression has been given by Paris and is known as Paris Law [9].

The expression represents a straight line when using logarithmic scales:

$\text{Log } N = \log a - m.\ \log(\Delta\ \sigma)$……………………………………..……..5

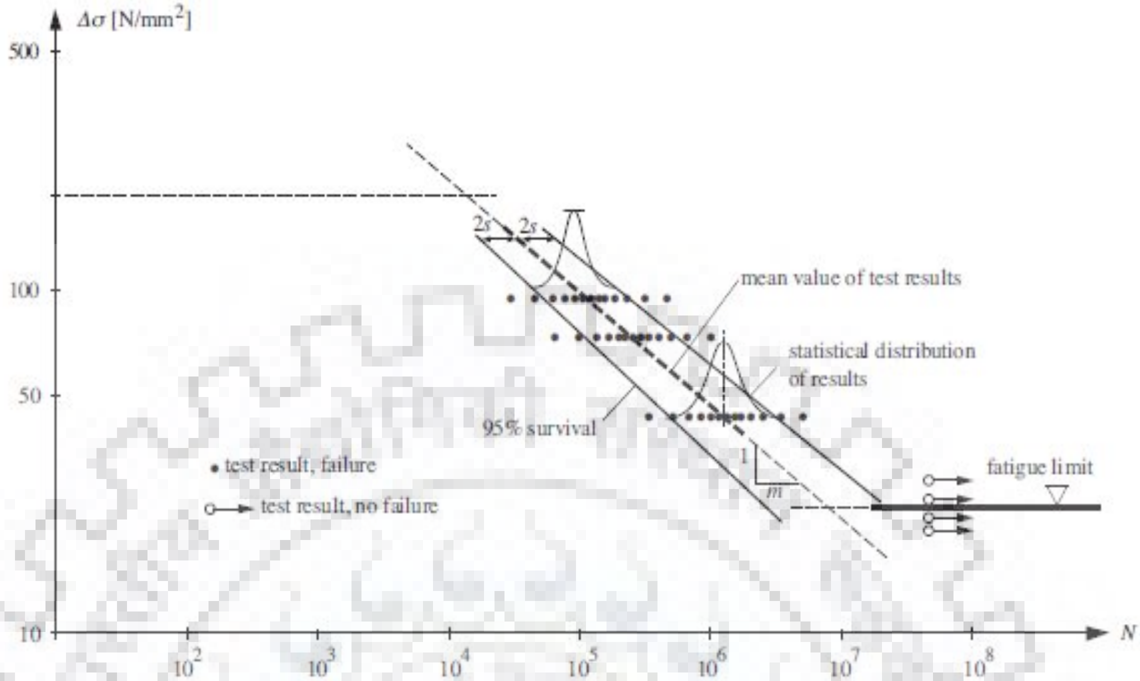

Figure 3. Fatigue test results for constant amplitude loading of structural steel members

The upper limit of the line i.e. higher Δσ values corresponds to twice the ultimate static strength of the material in reverse cyclic loading. The region with low number of cycles ranging between 10 and 10^4 is called low-cycle fatigue or oligo-cyclic fatigue shows large cyclic plastic deformations. The low-cycle fatigue strength is only relevant for loadings such as those occurring during earthquakes or silos where members experience only small numbers of stress cycles of high magnitude.

The lower limit of the line corresponding to low Δσ values represents the constant amplitude fatigue limit (CAFL), or endurance limit. This limit indicates that cyclic loading with stress ranges under this limit can be applied large number of times (> 10^8) without resulting in a fatigue failure i.e. a wider band scatter observed near the fatigue limit resulting from the specimens which do not show failure also after a large number of load cycles and these are called as run-out Fig. 4 [9]. Also, for aluminum, no real fatigue limit can be seen and only a line with a very shallow slope having large value of the slope coefficient m. It is also important to know the fact that a fatigue limit can only be acknowledged with tests performed under constant amplitude loadings. In order to derive a fatigue strength curve for design, i.e. a characteristic curve, the scatter of the test results must be taken into account. To achieve this, a given survival probability limit must be set. In EN 1993-1-9, a characteristic curve is chosen to represent a 95% survival probability, calculated from the mean value of two-sided 75% tolerance limits of the mean. To obtain exact position of the curve the number of the available test results should be large enough. This influence may be accounted from the recommendations published by the International Institute of Welding (IIS/IIW) [10]. For a sufficiently large number of data points (>60) the survival probability is approximated a straight line parallel to the mean regression line of the test results, but it is located on left side of the mean line at a two standard deviation 2s distance (Fig. 3).

2.4 Fatigue strength curves for direct stress ranges

In previous topic we have studied that the statistical analysis of the test results for a specific structural detail is allowed to define one fatigue strength curve (Fig 4). Numerous fatigue tests programs done for different details in steel and have shown that the fatigue strength curves are more or less parallel. From this we can say that fatigue strength is only a function of the constant "a" eqn. 5, and this value is specific for each structural detail.

$$\text{Log } N = \log a - m. \log (\Delta \sigma) \quad \ldots\ldots\ldots\ldots\ldots\ldots\ldots\ldots\ldots\ldots\ldots\ldots\ldots 6$$

Since there are many different details and hence the number of the different strength curves. Hence all the different structural details in categories are classified with a corresponding set of fatigue strength curves.

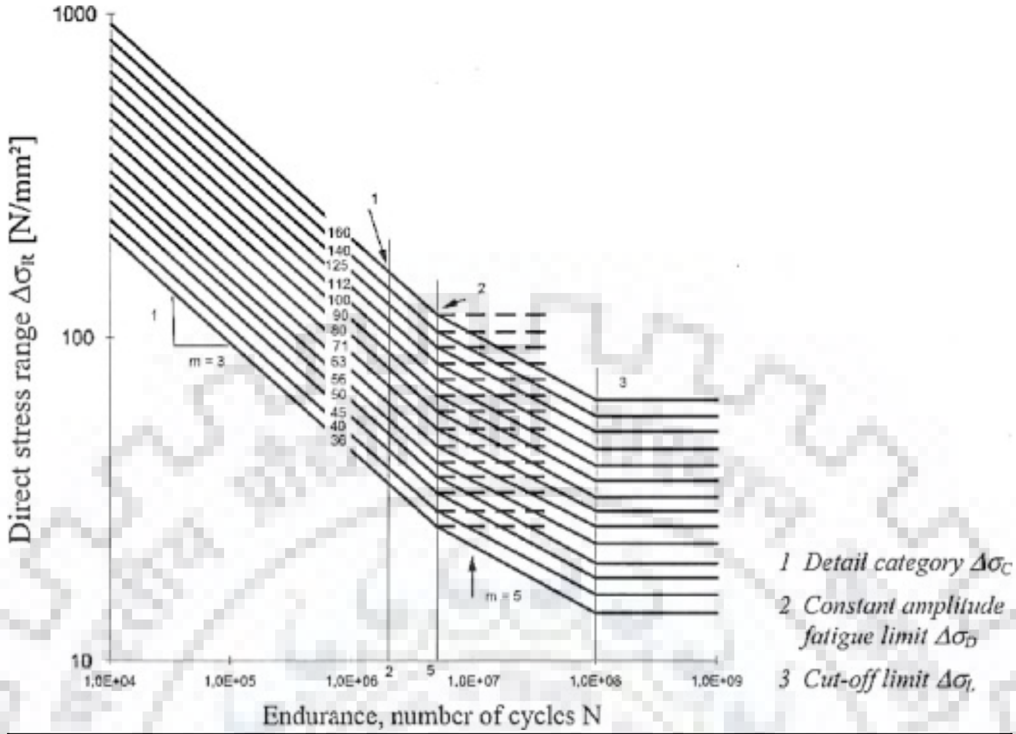

Figure 4. Set of fatigue strength curves for direct stress ranges

Classified structural details are described in different EN 1993 associated Eurocodes (EN 1993-1-9, EN 1993-2, EN 1993-3-2, etc.) but all of them refers to the same set of fatigue strength curves, as given in EC 1993 part 1-9. Each detail category corresponds to one S-N curve where the fatigue strength $\Delta\sigma$ is a function of the number of cycles, N where both are represented in logarithmic scale. There is a set is of fourteen S-N curves which are equally spaced in logarithmic scale as shown in Fig. 5. This set has been kept the same over the last decades and it comes from the ECCS first European recommendations [11]. The spacing between the curves corresponds to the difference in stress range of about 12% and values corresponding to the detail categories were rounded off [12].

All curves are characterized in 3 sections: (i) by the detail category, $\Delta\sigma_C$ (fatigue strength value at 2 million cycles in N/mm2), (ii) by the constant amplitude fatigue limit (CAFL), $\Delta\sigma_D$, at 5 million cycles representing about 74% of $\Delta\sigma_C$. For lives shorter than 5 million cycles the slope coefficient m is equal to 3. The fatigue life is infinity for constant amplitude stress ranges equal to or below CAFL. For all detail categories, the constant amplitude fatigue limit is fixed at 5 million cycles but this is not true for real fatigue behavior. The CAFL does not exist under variable amplitude loadings,. Thus there is a change in the slope coefficient to m = 5 between 5 million and 100 million of cycles. The last value corresponds to the cut-off limit, $\Delta\sigma_L$ corresponding to about 40% of $\Delta\sigma_C$. According to the definition, all the cycles with stress range equal to or below $\Delta\sigma_L$ can be neglected while performing damage sum. The reason for this is that the contribution of these stress ranges to the total damage is considered to be negligible.

It should be noted that the behavior under variable amplitude loading is complex. A few stress cycles can influence the start of a fatigue crack, even though the contribution of these cycles to the damage sum is negligible.

Note: Structural detail configuration for a type of structure can be found in the tables of the associated Eurocodes relevant to EN 1993 along with the description and requirements for the particular detail and with regards to that the fatigue strength can be known from the standard fatigue resistance S-N curves given in Eurocode 3 part 1-9.

Note: These fatigue curves are based on representative experimental investigations. They include the effects of:

- Stress concentrations due to the detail geometry (detail severity),
- Local stress concentrations due to the size and shape of weld imperfections within certain limits,
- Stress direction,
- Expected crack location,
- Residual stresses,
- Metallurgical conditions,
- Welding and post-welding procedures.

Also, stress concentrations due to geometry and other factors like misalignment, large cut-out in the vicinity of the detail are not included in the classified structural details [13].

2.5 Fatigue strength curves for shear stress ranges

For shear stress ranges, the statistical analysis of the test results for specific structural details have shown differences for fatigue cracks developing under shear with those under direct or normal stress ranges.

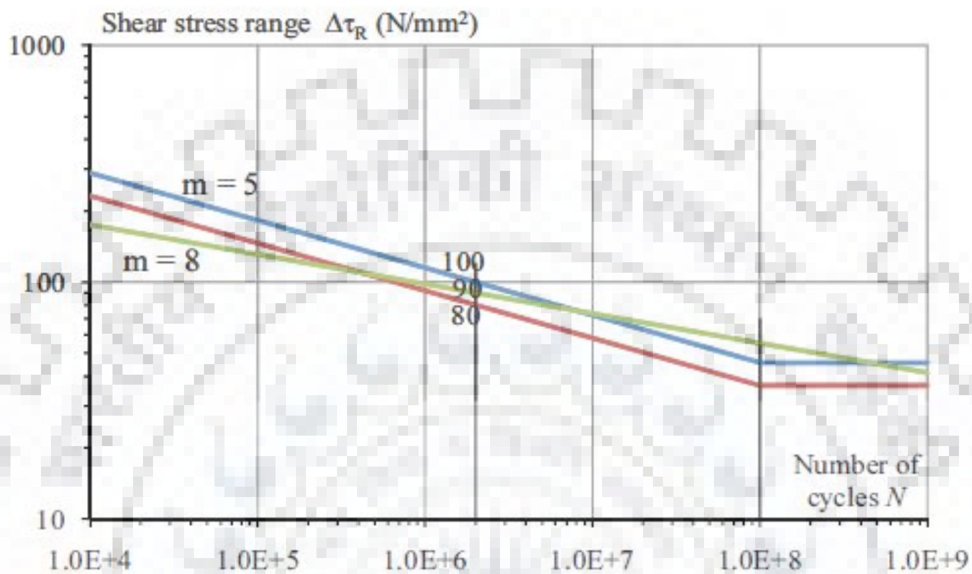

Figure 5. Set of fatigue strength curves for shear stress ranges

Firstly, the slope coefficient for fatigue strength curves for shear stress is higher than the curves under direct or normal stress ranges. Slope coefficient for shear stress ranges curve is m = 5. Secondly, there is no well-defined constant amplitude fatigue limit and thus the curve does not have CAFL. Thirdly, like other S-N curves, there is a cut-off limit at 100 million cycles.

2.6 Modified fatigue strength curve

The fatigue strength value for few details does not fit well in the original set of fatigue strength curves. Thus, there is a need to modify the curves. An example of one of the modified fatigue strength curves, category 45*, is represented in Fig. 6. The main difference lies in the location of the CAFL. The detail category is kept the same at 2 million cycles and also the slope coefficients but the CAFL as well as the slope change is located at 10 million cycles instead of 5 million cycles. As we know for lives more than 10 million cycles the slope coefficient m changes from 3 to 5, until 100 million cycles just before the cut-off limit.

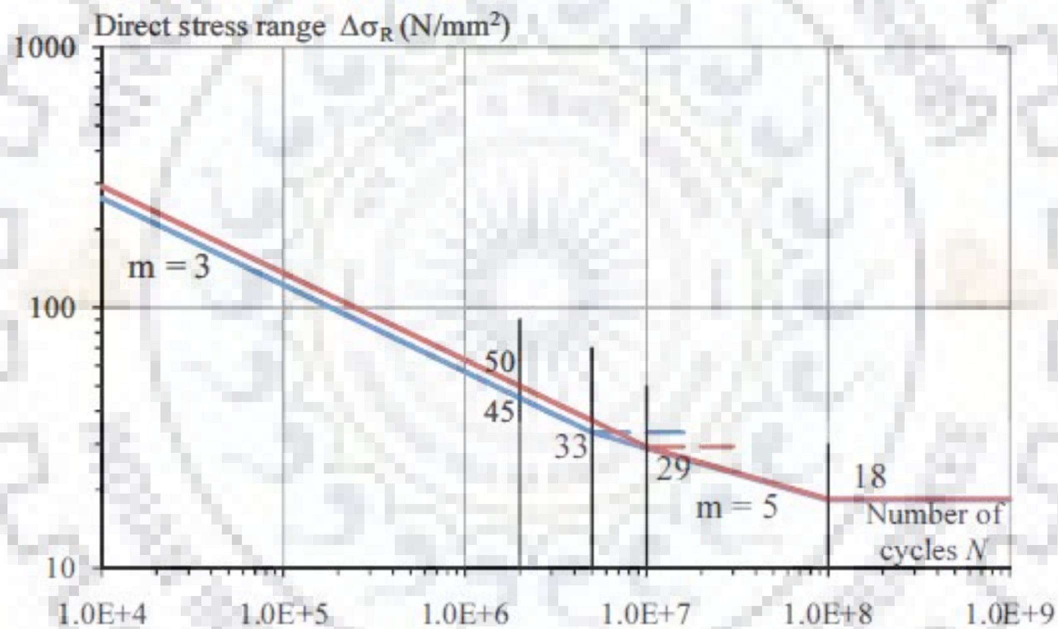

Figure 6. Alternative fatigue strength curves for a particular detail category 45*

With the rules given in EN 1993-1-9, the following two approaches can be chosen for such type of details:

- The detail category is put in the original set of curves but this results in a conservative approach when doing the verification with respect to fatigue strength at 2 million cycles. But it will result in a non-conservative verification if the CAFL is used.

- The detail category is put in the upper class, since it has an asterisk and the CAFL should be computed at 10 million cycles. This result in a lower CAFL value compared to the previous approach. The following equivalence can be written:

$\Delta\sigma_D$ (at 10 million cycles) = $(2/10)^{1/3}$ * 1.12 $\Delta\sigma_C$ *……………………………..7

In this case, the verification using the CAFL as well as the verification with respect to fatigue strength at 2 million cycles will be correct and more economical.

	Original curves [N/mm^2]			Alternative curves [N/mm^2]		
Category	$\Delta\sigma_C$	$\Delta\sigma_D$ at $5 \cdot 10^6$	$\Delta\sigma_L$	$\Delta\sigma_C$	$\Delta\sigma_D$ at 10^7	$\Delta\sigma_L$
36*	36	26.5	14.6	40	23.4	14.6
45*	45	33.2	18.2	50	29.2	18.2
56*	56	41.3	22.7	63	36.8	22.7

Table 1: Original and modified values of fatigue strength curves

One must be careful when using the first approach. For an example, one can look at an overlapped joint (detail 5, Table 8.5), which has a detail category 45*. This means that this detail can be conservatively classified as a category 45 detail. But, alternatively, it can also be classified as a category 50, providing that its CAFL is taken as $(2/10)^{1/3}$ 50 = 29 N/mm2 at 10 million cycles. Both classification cases are drawn for comparison in Fig. 6. The values of the conservative and alternative classifications given in EN 19931-9 are summarized in Table 1.

Chapter 3 STATISTICAL INTERVALS

3.1 Regression Analysis

$\Delta\sigma$ and N for stress ranges $\Delta\sigma$ above the fatigue limit on a double logarithmic scale.

Log N = log a – m. log $\Delta\sigma$ + Ɛ………………………………….8

Where,

Log N……… log (base 10) of corresponding number of cycles to failure N

Log a………. Intercept on the n axis

m………….... Slope of $\Delta\sigma$-N curve linear on a log- log basis

Log $\Delta\sigma$ ……..log (base 10) of stress range $\Delta\sigma$ allowable.

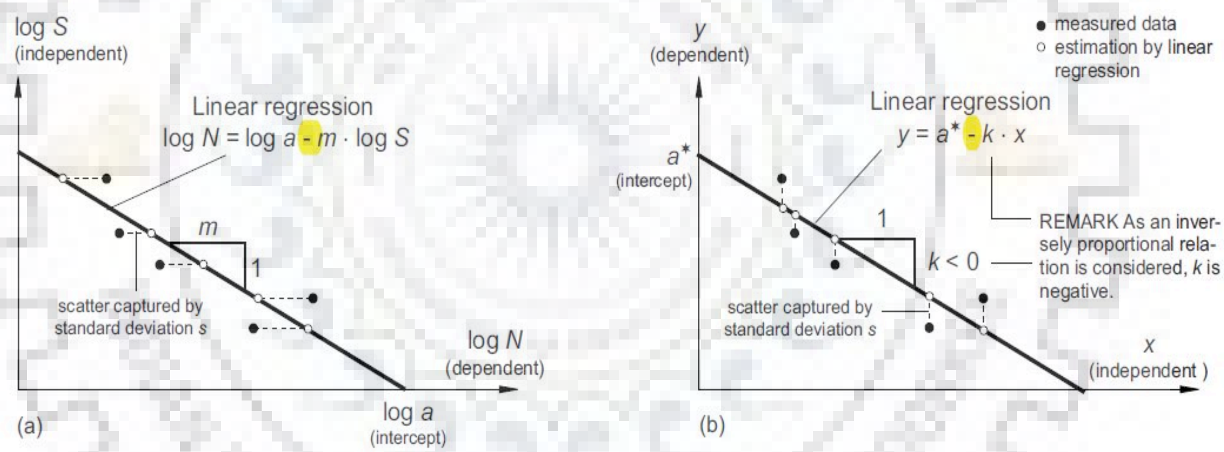

Figure 7. Linear regression (a) in fatigue (b) in mathematics and statistics

The laws of mathematics states that the independent variable is plotted on horizontal axis and the dependent variable is plotted on vertical axis, while in engineering science with respect to fatigue it is vice versa as shown in Fig 7. Also, the mathematical rules used to derive the intercept with the axis of the dependent variable, the slope of the regression line ($\Delta\sigma$-N curve), the standard deviation used all have to be adjusted respectively. The positive slope m used in fatigue is identical to the negative inverse of the mathematical gradient of the regression line ($\Delta\sigma$-N curve), m = -1/k.

Table 2: Methods for the statistical analysis of fatigue test results

Method	-*N* Curve Equation	Method and Assumptions	Parameter
1	log *N* = log a – m log	Linear regression of log *N* on log and log on log *N* , ignoring run-outs, mean line bisecting the two regression lines.	*C, m, p(log N)*
2	log *N* = log a – m log	Linear regression of log *N* on log , ignoring run-outs.	*C, m, p(log N)*
3	log *N* = log a – m log	Maximum likelihood, including run-outs.	*C, m, p(log)*
4	log *N* = log a – m log	Linear regression of log *N* on log , ignoring run-outs.	*C, m, p(log)*
5		Multiple non-linear regression including censored data (run-outs)	*A, B, E, p()*

$m=n.i(\log\Delta\sigma i-\log Ni)-i\log\Delta\sigma i\ .\ i\log Nin.\ i(\log\Delta\sigma i)2-i\log\Delta\sigma i2$

-----------------------9

i……… number of single test data

n……… sample size

For the intercept log a of the regression line on the log axis it holds:

$\log a= 1n.\ i\log Ni+m.\ i\log\Delta\sigma i$ ----------------------------------10

Since the regression line only includes finite life span, run-outs and data points with more than 5

3.2 Two sided statistical intervals, one-sided statistical bounds

The regression line defines an average relationship of $\Delta\sigma$ and N based on sampled data.

Fig. 8(a)

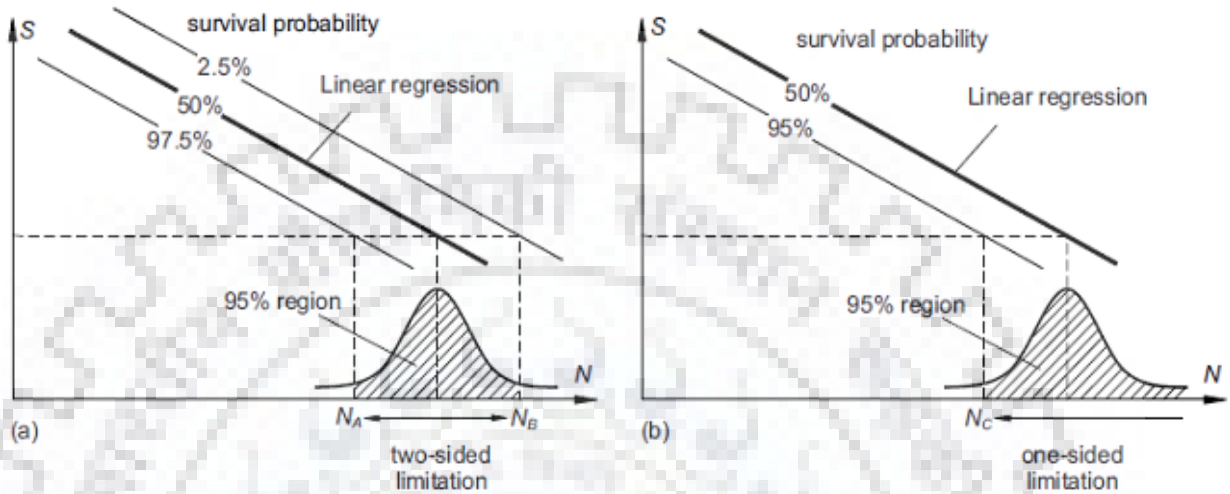

Figure 8. (a) Two sided statistical intervals, (b) one-sided statistical bounds of the fatigue life N predicted by the regression line for a particular stress range $\Delta\sigma$

3.3 Statistical Interval

From the statistical point of view, there are three different types of statistical intervals of the mean regression line that can be derived from the sampled data. The appropriate interval depends upon particular application. The three different intervals frequently used are: -

1. Confidence Intervals
2. Tolerance Intervals
3. Prediction Intervals

3.3.1 Confidence Interval:

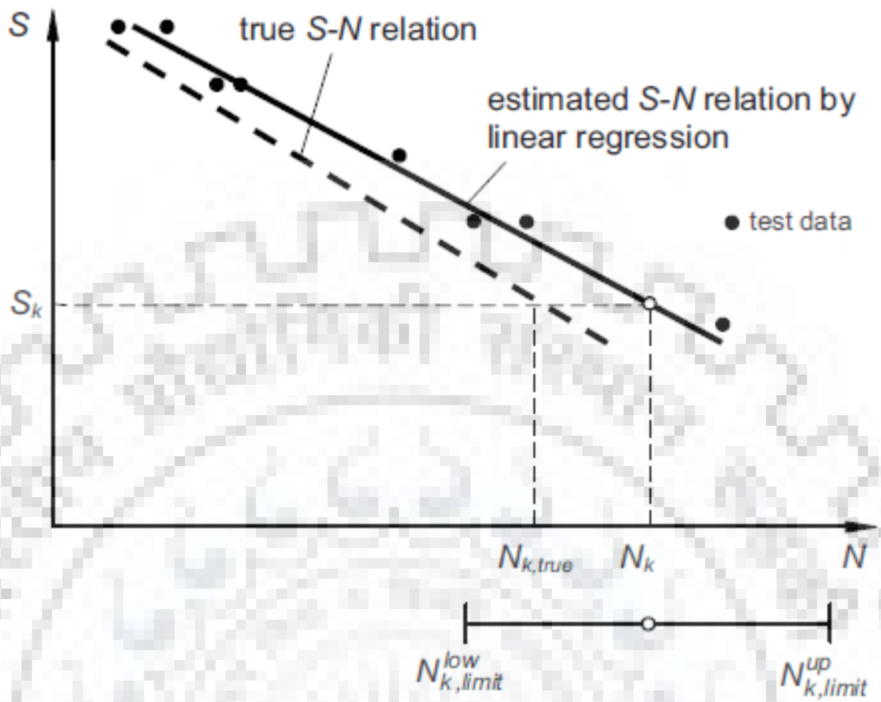

Figure 9. Confidence interval of the mean regression line

log N_k can be computed by Eq. 10 [15] [16].the one-sided 100(1 − α) % lower confidence bound will be identical with the lower limit of a two-sided 100(1 − 2α)% confidence interval

Two-sided 100 $(1-\alpha)$% confidence interval:

$\log Nk,limit = \log Nk \pm t\alpha 2,dof.\text{p. } 1n+ \log \Delta\sigma k - \log \Delta\sigma 2i \log \Delta\sigma i - \log \Delta\sigma 2$

……………11

One-sided 100 $(1-\alpha)$% confidence interval:

$\log Nk,limit = \log Nk - ta,dof.\text{p. } 1n+ \log \Delta\sigma k - \log \Delta\sigma 2i \log \Delta\sigma i - \log \Delta\sigma 2$

…………..12

Where,

Log $\Delta\sigma_k$ ……………..Considered Stress range

Log N_k ………………Value of N predicted by mean regression line for $\Delta\sigma = \Delta\sigma$

$_k$.

Log $\Delta\sigma$ ……………. ..Mean value of Sampled log $\Delta\sigma$.

p……………………. . Standard deviation of sampled log N from the mean regression line.

t…………………….. Co-efficient of student-t distribution.

α……………………. Significance level.

Dof ………………… Degree of Freedom.

n……………………. Sample size.

The Variation between the sampled values of log N and those predicted by the mean regression line is obtained by the standard deviation p of the sample:

p= i logNi−(log$a$−$m$log$\Delta\sigma i$2 dof

…………….13

3.3.2 Tolerance Interval:

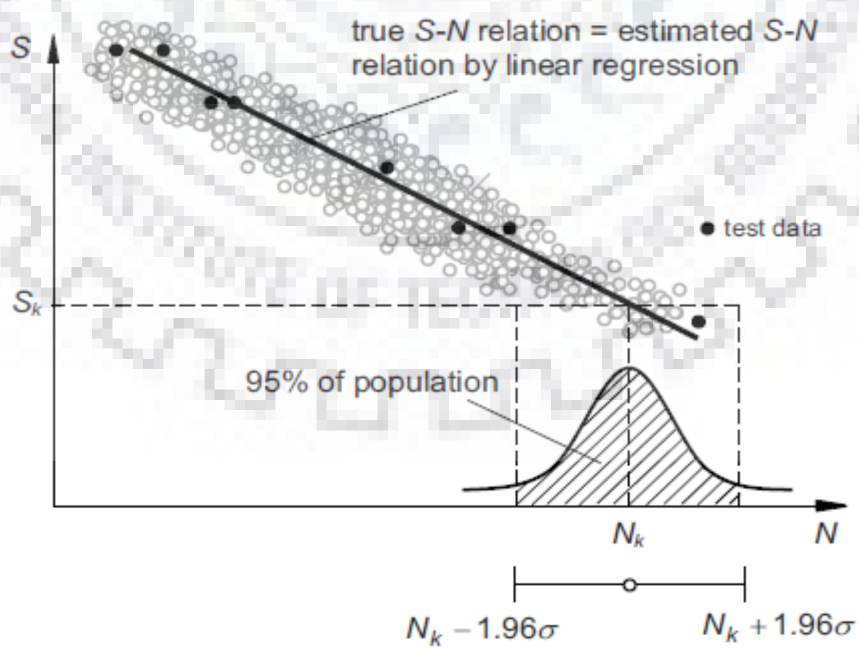

Figure 10.Tolerance interval of the mean regression line containing 95% of the population

it means all existing structures have been tested, the sample error will disappear and the one-sided tolerance bound will coincide with the lower limit of Eq. 12.

$\log N k{,}limit = \log N k - k P{,}1-a.\text{p. } 1n+1+ \log \Delta\sigma k - \log \Delta\sigma 2 i \log \Delta\sigma i - \log \Delta\sigma 2$

…………14

Where,

Log $\Delta\sigma_k$ ……………Considered Stress range

Log N_k ……………. Value of N predicted by mean regression line for $\Delta\sigma = \Delta\sigma_k$.

Log $\Delta\sigma$ ……………..Mean value of Sampled log $\Delta\sigma$.

p……………………. Standard deviation of sampled log N from the mean regression line.

Dof ………………… Degree of Freedom.

N……………………. Sample size.

A……………………. Significance level.

$K_{p,\,1-\alpha}$ ………………... Coefficient.

$1 - \alpha$ ………………... Confidence level

P ……………………. Proportion to be contained by the interval.

3.3.3 Prediction Interval:

Where,

Log $\Delta\sigma_k$ …………….. Considered Stress range

Log N_k ……………. Value of N predicted by mean regression line for $\Delta\sigma = \Delta\sigma_k$.

Log $\Delta\sigma$……………… Mean value of Sampled log $\Delta\sigma$.

p……………………. standard deviation of sampled log N from the mean regression line.

t…………………….. Co-efficient of student-t distribution.

α……………………. Significance level.

Dof ………………… Degree of Freedom.

n……………………. Sample size.

The one-sided 100(1 − α) % lower prediction bound will be identical with the lower limit of a two-sided 100(1 − 2α) % prediction interval.

As the prediction interval has to account for the uncertainty of future sampling they must be wider than a confidence interval. In contrast to the confidence interval its width does not reduces to zero if the sample size becomes infinitive.

3.4 Test data significance:

Generally the fatigue strength curves are evaluated from series of fatigue tests performed on specimens, which typically reproduces the detail to be studied. For each series, a fatigue strength curve (or $\Delta\sigma$ -N curve) can be most accurately determined when groups of fatigue specimens are tested at different stress range levels. However, no internationally recognized method of fatigue testing and design of experiments are being agreed upon. In that respect, the fatigue test data found in the literature are somewhat non homogeneous.

- statistically to sufficient confidence in the interpretation of the results.

In order to have a consistent method of comparison between fatigue test results of various details, a common statistical analysis procedure has been applied systematically to each individual set of fatigue test results [18].

3.4.1 Test analysis procedure:

For the statistical evaluation, only test data with number of load cycles to failure criteria comprised between 10^4 and $5*10^6$ cycles are considered. Rather than taking a lower bound limit approach for each detail, a statistical evaluation of the fatigue data was performed on each of the groups. Generally the fatigue test results are scattered when plotted on a log-log scale.

The statistical evaluation proceeds in two different steps:

- A linear regression analysis with both variable and fixed slope constant values
- And an evaluation of the characteristic fatigue strength at $2*10^6$ cycles.

It has been considered, that there are existing different definitions of characteristic fatigue strength curves in the codes in Europe for example, Eurocode 3 part 1-9 requires 75% confidence level of 95% probability of survival for log (N) test data, accounting for standard deviation and sample size and Background Documentation of Eurocode 3 requires One-sided confidence interval with a lower limit defining a 95% probability of survival for log (N) test data i.e. one-sided 95% prediction bound [18].

3.4.2 Linear regression analysis:

Log N = log a – m. log $\Delta\sigma$ ……….…………………………………….17

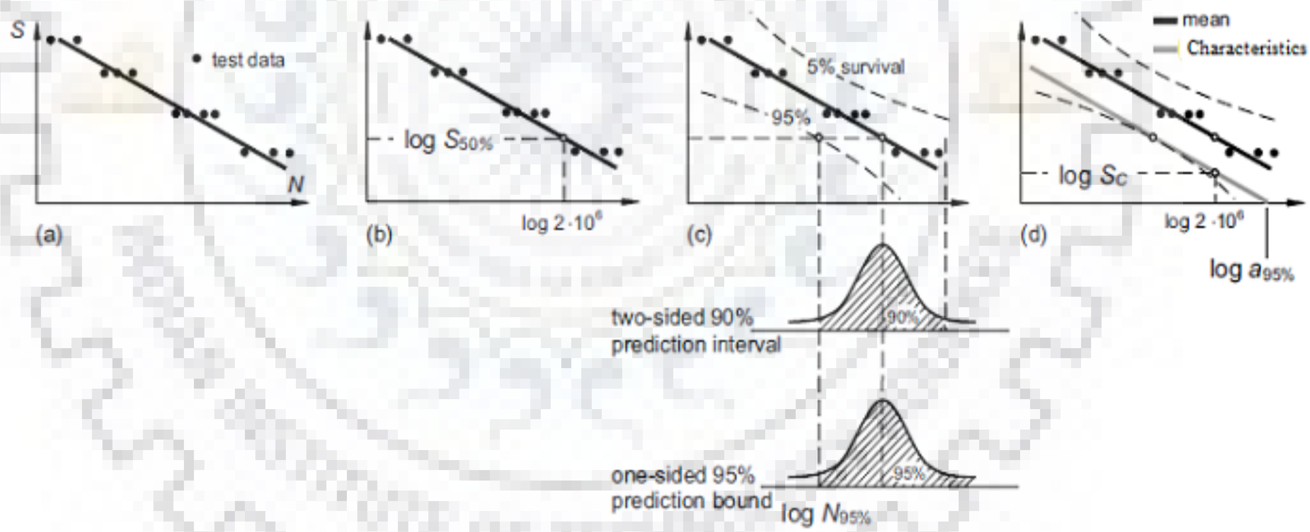

Figure 11. Evaluation according to background documentation 9.01: (a) linear regression, (b) analysis of regression line, (c) Prediction interval, (d) reference value of fatigue strength

3.4.3 Analysis of Regression line:

3.4.4 Prediction Interval:

3.4.5 Reference value of fatigue strength:

3.5 Comparison of the intervals

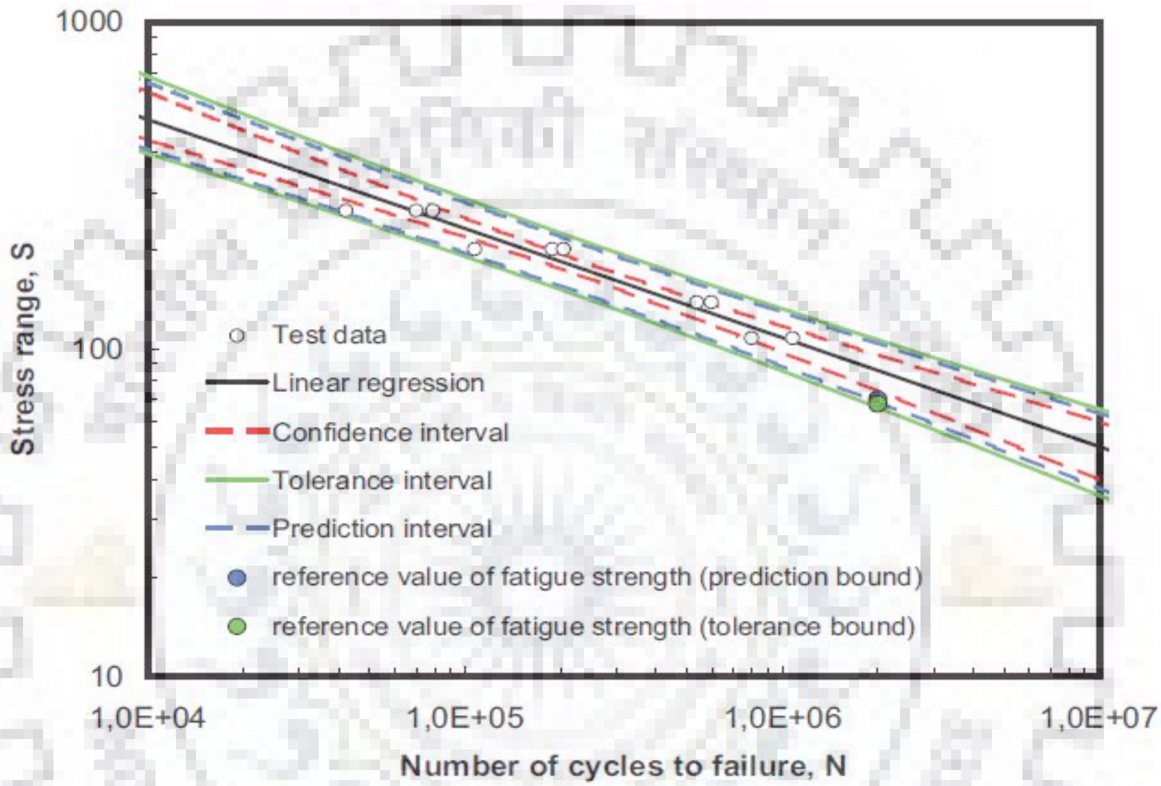

Figure 12. Comparison of all three intervals

If the number of test data is increased then the value of one-sided lower prediction bound becomes quite similar to the value of one- sided tolerance bound i.e. large sample size increases statistical stability.

Chapter 4 RE-EVALUATION OF EXISTING FATIGUE CODES

4.1 Introduction

As already being discussed in Section 2.4 that the fatigue strength is represented by series of S-N curves for normal stress ranges and shear stress ranges which represent a typical detail categories. Each detail category is designated by a number, which represents the reference value of the fatigue strength in N/mm^2 for direct stress ranges and shear stress ranges at 2 million cycles.

Detail categories for direct stress ranges and shear stress ranges for different type of attachments and joints are given in Eurocode 3.1-9 in different tables as listed below:

- Table 8.1 for plain members and mechanically fastened joints
- Table 8.2 for welded built-up sections
- Table 8.3 for transverse butt welds
- Table 8.4 for weld attachments and stiffeners
- Table 8.5 for load carrying welded joints
- Table 8.6 for hollow sections
- Table 8.7 for lattice girder node joints
- Table 8.8 for orthotropic decks - closed stringers
- Table 8.9 for orthotropic decks open stringer
- Table 8.10 for top flange to web junctions of runway beams.

Research has been done on Detail 5 and Detail 6 given in Table 8.5 shown below i.e. the load carrying fillet welds. Detail 5 geometry consists of overlapped fillet welded lapped joint with a detail category of 45* N/mm^2 while Detail 6 geometry consists of cover plates welded on beam flanges and plate girders with different values of detail category depending upon the thickness of the flanges and the cover plates. Maximum value of detail category for detail 6 is 56* N/mm^2, and decreases with the increase in the thickness of the flange and the cover plate.

In detail 6 end zones of single and multiple welded cover plates were acknowledged with both with and without transverse end welds. If the cover plate is wider than the flange then it is necessary to weld the cover plate transversely at the end and the weld should be carefully ground to remove undercuts. Table 8.5 is given below:

Table 2a: EC 3.1-9, Table 8.5: Load carrying Fillet welds

AC2 Detail category	Constructional detail			Description	Requirements
80	$\ell<50$ mm	all t [mm]	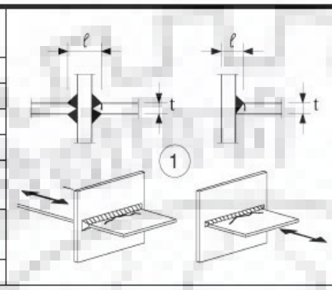	Cruciform and Tee joints: 1) Toe failure in full penetration butt welds and all partial penetration joints.	1) Inspected and found free from discontinuities and misalignments outside the tolerances of EN 1090. 2) For computing $\Delta\sigma$, use modified nominal stress. 3) In partial penetration joints two fatigue assessments are required. Firstly, root cracking evaluated according to stresses defined in section 5, using category 36* for $\Delta\sigma_w$ and category 80 for $\Delta\tau_w$. Secondly, toe cracking is evaluated by determining $\Delta\sigma$ in the load-carrying plate. Details 1) to 3): The misalignment of the load-carrying plates should not exceed 15 % of the thickness of the intermediate plate.
71	$50<\ell\le80$	all t			
63	$80<\ell\le100$	all t			
56	$100<\ell\le120$	all t			
56	$\ell>120$	$t\le20$			
50	$120<\ell\le200$ $\ell>200$	$t>20$ $20<t\le30$			
45	$200<\ell\le300$ $\ell>300$	$t>30$ $30<t\le50$			
40	$\ell>300$	$t>50$			
As detail 1 in Table 8.5	flexible panel 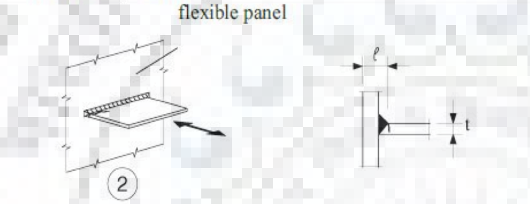			2) Toe failure from edge of attachment to plate, with stress peaks at weld ends due to local plate deformations.	
36*	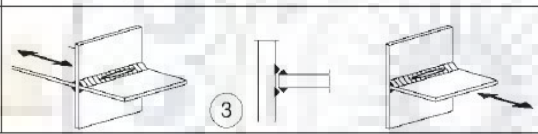			3) Root failure in partial penetration Tee-butt joints or fillet welded joint and in Tee-butt weld, according to Figure 4.6 in EN 1993-1-8:2005. AC2	

Table 2b: EC 3.1-9, Table 8.5: Load carrying Fillet welds

As detail 1 in Table 8.5	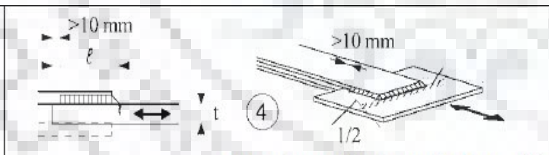stressed area of main panel: slope = 1/2			Overlapped welded joints: 4) Fillet welded lap joint.	4) $\Delta\sigma$ in the main plate to be calculated on the basis of area shown in the sketch. 5) $\Delta\sigma$ to be calculated in the overlapping plates. Details 4) and 5): - Weld terminations more than 10 mm from plate edge. - Shear cracking in the weld should be checked using detail 8).
45*	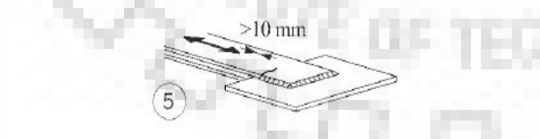			Overlapped: 5) Fillet welded lap joint.	
	$t_c<t$	$t_c\ge t$	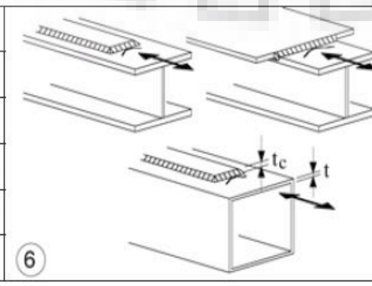	Cover plates in beams and plate girders: 6) End zones of single or multiple welded cover plates, with or without transverse end weld.	6) If the cover plate is wider than the flange, a transverse end weld is needed. This weld should be carefully ground to remove undercut. The minimum length of the cover plate is 300 mm. For shorter attachments size effect see detail 1).
56*	$t\le20$	-			
50	$20<t\le30$	$t\le20$			
45	$30<t\le50$	$20<t\le30$			
40	$t>50$	$30<t\le50$			
36	-	$t>50$			

Statistical analysis of the sources collected on the basis of geometry and type of welds for detail 5 & detail 6 was done. Eurocode 3.1-9 requires formally one sided 95% tolerance bound while we have done the statistical analysis on the basis of one sided 95% prediction bound.

Table 2c: EC 3.1-9, Table 8.5: Load carrying Fillet welds

56	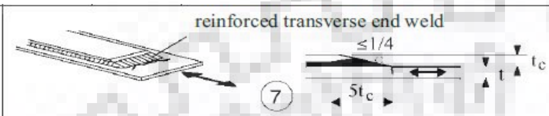	7) Cover plates in beams and plate girders. $5t_c$ is the minimum length of the reinforcement weld.	7) Transverse end weld ground flush. In addition, if $t_c > 20$mm, front of plate at the end ground with a slope < 1 in 4.
80 m=5	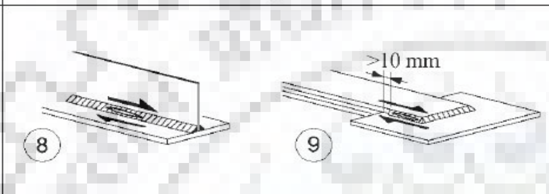	8) Continuous fillet welds transmitting a shear flow, such as web to flange welds in plate girders. 9) Fillet welded lap joint.	8) $\Delta\tau$ to be calculated from the weld throat area. 9) $\Delta\tau$ to be calculated from the weld throat area considering the total length of the weld. Weld terminations more than 10 mm from the plate edge, see also 4) and 5) above.
see EN 1994-2 (90 m=8)	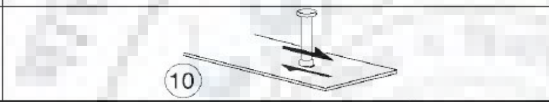	Welded stud shear connectors: 10) For composite application	10) $\Delta\tau$ to be calculated from the nominal cross section of the stud.
71	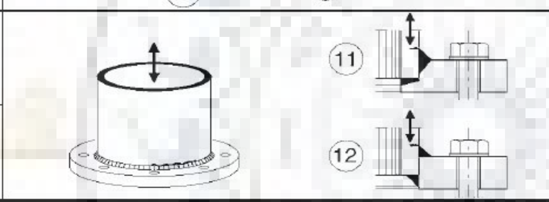	11) Tube socket joint with 80% full penetration butt welds.	11) Weld toe ground. $\Delta\sigma$ computed in tube.
40		12) Tube socket joint with fillet welds.	12) $\Delta\sigma$ computed in tube.

For the evaluation of the details both statistically and source quality, data has been collected from the sources listed below for detail 5 and detail 6.

Table 3: List of sources for table 8.5: Detail 5

12	Japanese Society Of Steel Construction (JSSC)	Fatigue Design Recommendations for Steel Structures	2_4_JSSC 13
18	Gurney T.R., Maddox S.J.	A Re-Analysis of Fatigue Data for Welded Joints in Steel	3_5_LCW 6
113	Macfarlane D.S., Harrison J.D.	Some fatigue tests of load-carrying transverse fillet welds	6_19
113	Macfarlane D.S., Harrison J.D.	Some fatigue tests of load-carrying transverse fillet welds	6_20
113	Macfarlane D.S., Harrison J.D.	Some fatigue tests of load-carrying transverse fillet welds	6_21
113	Macfarlane D.S., Harrison J.D.	Some fatigue tests of load-carrying transverse fillet welds	6_22
113	Macfarlane D.S., Harrison J.D.	Some fatigue tests of load-carrying transverse fillet welds	6_23
133	Webber D.	The comparison of the fatigue strength of welded joints in structural steel made at Sheff	6_27
133	Webber D.	The comparison of the fatigue strength of welded joints in structural steel made at Sheff	6_28
133	Webber D.	The comparison of the fatigue strength of welded joints in structural steel made at Sheff	6_29
91	Baxter D.E., Modlen G.F.	Some factors affecting the fatigue strength of fillet welds	6_32
91	Baxter D.E., Modlen G.F.	Some factors affecting the fatigue strength of fillet welds	6_33
91	Baxter D.E., Modlen G.F.	Some factors affecting the fatigue strength of fillet welds	6_34
91	Baxter D.E., Modlen G.F.	Some factors affecting the fatigue strength of fillet welds	6_35
91	Baxter D.E., Modlen G.F.	Some factors affecting the fatigue strength of fillet welds	6_36
91	Baxter D.E., Modlen G.F.	Some factors affecting the fatigue strength of fillet welds	6_37
91	Baxter D.E., Modlen G.F.	Some factors affecting the fatigue strength of fillet welds	6_38
91	Baxter D.E., Modlen G.F.	Some factors affecting the fatigue strength of fillet welds	6_39
91	Baxter D.E., Modlen G.F.	Some factors affecting the fatigue strength of fillet welds	6_40
91	Baxter D.E., Modlen G.F.	Some factors affecting the fatigue strength of fillet welds	6_41
91	Baxter D.E., Modlen G.F.	Some factors affecting the fatigue strength of fillet welds	6_42
91	Baxter D.E., Modlen G.F.	Some factors affecting the fatigue strength of fillet welds	6_43
91	Baxter D.E., Modlen G.F.	Some factors affecting the fatigue strength of fillet welds	6_44
91	Baxter D.E., Modlen G.F.	Some factors affecting the fatigue strength of fillet welds	6_45
91	Baxter D.E., Modlen G.F.	Some factors affecting the fatigue strength of fillet welds	6_46
95	Brine F.E., Webber D., Baron H.G.	Effect of shot peening on the fatigue properties of maraging steel and Al-Zn-Mg alloy	6_54
95	Brine F.E., Webber D., Baron H.G.	Effect of shot peening on the fatigue properties of maraging steel and Al-Zn-Mg alloy	6_55

Table 4: List of sources for table 8.5: Detail 6

Übersicht: Table 8-5: 6			
141	Hirt M.A., Crisinel M.	La resistance a la fatigue des pontres en ame pleine composees-soudees, Effect d	3_4_NLC 13
29	Fisher J.W., Albrecht P.A., Yen B.T., Klingerman D.J., Mc Namee B.M.	Fatigue strength of steel beams with welded stiffeners and attachments	3_4_NLC 22
29	Fisher J.W., Albrecht P.A., Yen B.T., Klingerman D.J., Mc Namee B.M.	Fatigue strength of steel beams with welded stiffeners and attachments	3_4_NLC 23
29	Fisher J.W., Albrecht P.A., Yen B.T., Klingerman D.J., Mc Namee B.M.	Fatigue strength of steel beams with welded stiffeners and attachments	3_4_NLC 24
29	Fisher J.W., Albrecht P.A., Yen B.T., Klingerman D.J., Mc Namee B.M.	Fatigue strength of steel beams with welded stiffeners and attachments	3_4_NLC 25
18	Gurney T.R., Maddox S.J.	A Re-Analysis of Fatigue Data for Welded Joints in Steel	3_5_LCW 1
18	Gurney T.R., Maddox S.J.	A Re-Analysis of Fatigue Data for Welded Joints in Steel	3_5_LCW 2
18	Gurney T.R., Maddox S.J.	A Re-Analysis of Fatigue Data for Welded Joints in Steel	3_5_LCW 3
28	Fisher J.W., Frank K.H., Hirt M.A., Mc Namee B.M.	Effect of weldments on the fatigue of steel beams	3_5_LCW 11
28	Fisher J.W., Frank K.H., Hirt M.A., Mc Namee B.M.	Effect of weldments on the fatigue of steel beams	3_5_LCW 12
28	Fisher J.W., Frank K.H., Hirt M.A., Mc Namee B.M.	Effect of weldments on the fatigue of steel beams	3_5_LCW 13
28	Fisher J.W., Frank K.H., Hirt M.A., Mc Namee B.M.	Effect of weldments on the fatigue of steel beams	3_5_LCW 14
85	Schilling C. G., Klipstein K. H., Barsom J. M., Blake G.T.	Fatigue of Welded Steel Bridge Members Under Variable Amplitude Loadings	3_5_LCW 15
85	Schilling C. G., Klipstein K. H., Barsom J. M., Blake G.T.	Fatigue of Welded Steel Bridge Members Under Variable Amplitude Loadings	3_5_LCW 16
28	Fisher J.W., Frank K.H., Hirt M.A., Mc Namee B.M.	Effect of weldments on the fatigue of steel beams	3_5_LCW 17
28	Fisher J.W., Frank K.H., Hirt M.A., Mc Namee B.M.	Effect of weldments on the fatigue of steel beams	3_5_LCW 17a
28	Fisher J.W., Frank K.H., Hirt M.A., Mc Namee B.M.	Effect of weldments on the fatigue of steel beams	3_5_LCW 18
28	Fisher J.W., Frank K.H., Hirt M.A., Mc Namee B.M.	Effect of weldments on the fatigue of steel beams	3_5_LCW 19
28	Fisher J.W., Frank K.H., Hirt M.A., Mc Namee B.M.	Effect of weldments on the fatigue of steel beams	3_5_LCW 20
28	Fisher J.W., Frank K.H., Hirt M.A., Mc Namee B.M.	Effect of weldments on the fatigue of steel beams	3_5_LCW 21
85	Schilling C. G., Klipstein K. H., Barsom J. M., Blake G.T.	Fatigue of Welded Steel Bridge Members Under Variable Amplitude Loadings	3_5_LCW 22
29	Fisher J.W., Albrecht P.A., Yen B.T., Klingerman D.J., Mc Namee B.M.	Fatigue strength of steel beams with welded stiffeners and attachments	7_137
29	Fisher J.W., Albrecht P.A., Yen B.T., Klingerman D.J., Mc Namee B.M.	Fatigue strength of steel beams with welded stiffeners and attachments	7_138
29	Fisher J.W., Albrecht P.A., Yen B.T., Klingerman D.J., Mc Namee B.M.	Fatigue strength of steel beams with welded stiffeners and attachments	7_139
29	Fisher J.W., Albrecht P.A., Yen B.T., Klingerman D.J., Mc Namee B.M.	Fatigue strength of steel beams with welded stiffeners and attachments	7_140

Total numbers of sources that have been listed in the commentary for the evaluation of detail 5 are 6 amongst which source number 133 is not available. Whereas total number of sources listed for detail 6 are 5 among this source number 85 entitled “fatigue of welded steel bridge members under variable amplitude loadings” is not been analyzed because of absence of constant amplitude.

In above table the first column designates to the source ID number that has been assigned to the particular source, second column represents the author name followed by the source title in the third column while the last column represents the series number that has been allotted to the sources in the commentary a background document that has been developed in support to the implementation, harmonization and further development in the Eurocodes.

Data in the database file has been collected from the given sources. Database file consist of 7 different sections which are listed below:

- General information
    - Series name
    - Sub series name
    - Source ID1, ID2…
    - Remarks if any,
    - Series part of commentary EC 3.1-9 (Y/N)
- Loading conditions
    - Kind of loading
    - Constant amplitude (Y/N)
    - Low frequency value (Hz)
    - High frequency value (Hz)
    - Location of calculated stress amplitude.
- Material properties
    - Part 1(Web/ flange/cover plate)
    - Steel grade1
    - Low yield strength 1 [MPa]
    - High yield strength 1 [MPa]
    - Low tensile strength 1 [MPa]

- High tensile strength 1 [MPa], so on part 2, part 3…

➢ Welding conditions
  - Weld shape
  - Elementary weld symbol as per given in EN ISO 2553
  - Number of passes group I, II, III
  - Welding process I, II, III
  - Weld pretreatment part 1, part 2, part 3
  - Weld post treatment part 1, part 2, part 3
  - Continuous weld group I, II, III
  - Filler material group I
    - Low yield strength of filler material group I [MPa]
    - High yield strength of filler material group I [MPa]
    - Low tensile strength of filler material group I [MPa]
    - High tensile strength of filler material group I [MPa], So on for group II, III

➢ Environmental conditions
  - Low temperature [°C]
  - High temperature [°C]
  - Corrosive conditions
  - Humidity
  - Irradiation

➢ Previous evaluation (DASt-data)

➢ Detail specific properties

➢ Tests results
  - Single test information available (Y/N)
  - Stress ratio [R]
  - Nominal stress amplitude [MPa]
  - Cycles to failure N0; unknown failure criterion
  - Cycles to failure N1; number of cycles at 5% change in strain near the point of initiation
  - Cycles to failure N2; number of cycles at detection of crack

- Cycles to failure N3; number of cycles at through thickness cracking
- Cycles to failure N4; number of cycles at complete loss of strength
- Cycles to failure N5; else, remark
- Cycles until failure N6; number of cycles until end of test without failure of specimen (runout)
- Runout (Y/N)
- Failure region
- Remarks, if any

4.2 Source evaluation criteria

In background document EC 3.1-9, criteria used to define good quality source for evaluation depends on many factors but only four factors are being taken into account. These are:

- Source available and verified: Available source should be verified.
- Single test data available: This means that the test results can either be given in tabular form or graphical form. Tabular data gives more accurate statistical results.
- Number of single test: For more accurate statistical results number of test should be more than 10.
- Failure region available: Failure criteria and region of failure should be known.

Table 5: Criteria used for source evaluation

Criterion	Evaluation
Source available and verified?	Yes
	No
Single test data available?	Yes
	graphical
	No
Number of single tests	≥ 10
	≥ 7
	< 4
Failure criterion known?	Yes
	No

As we are dealing with welded structures, the other parameters do not have much influence on fatigue for steel structure. Also, the types of steel used do not have any influence on fatigue, as it does not depend on the strength of the base material in case of welded structure.

4.3 Evaluation of detail 5

Statistical results of all of series of detail 5 are given below. There are total 6 sources and 27 series available for the evaluation.

4.3.1 Statistical evaluation of Source 19

Series that belongs to source ID number 19 is 2_4_JSSC 13. Title of the source is "Fatigue design recommendations for steel structures" given by Japanese society of steel construction. The specimen consist of fillet welded lapped joint, welded on all the three sides of the cover plate as shown in Fig. 13. Tests were performed under constant amplitude loadings and not much information about the steel grade and welding information is not given. Test data are available in graphical form shown in Fig. 14.

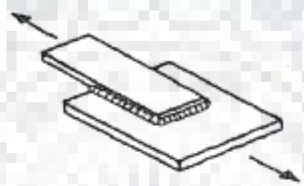

Figure 13a. Specimen with fillet weld lap joint

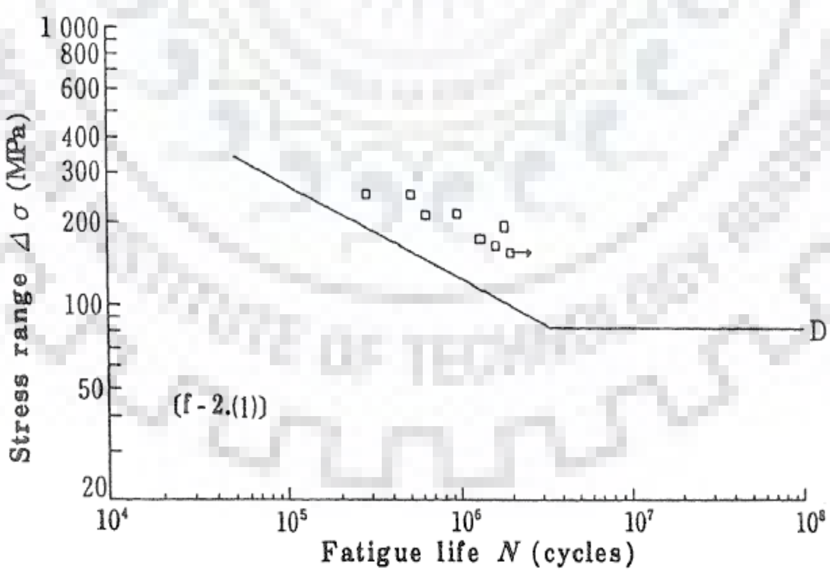

Figure 13b. S-N curve for Source 12, Series 2-4-JSSC 13[19]

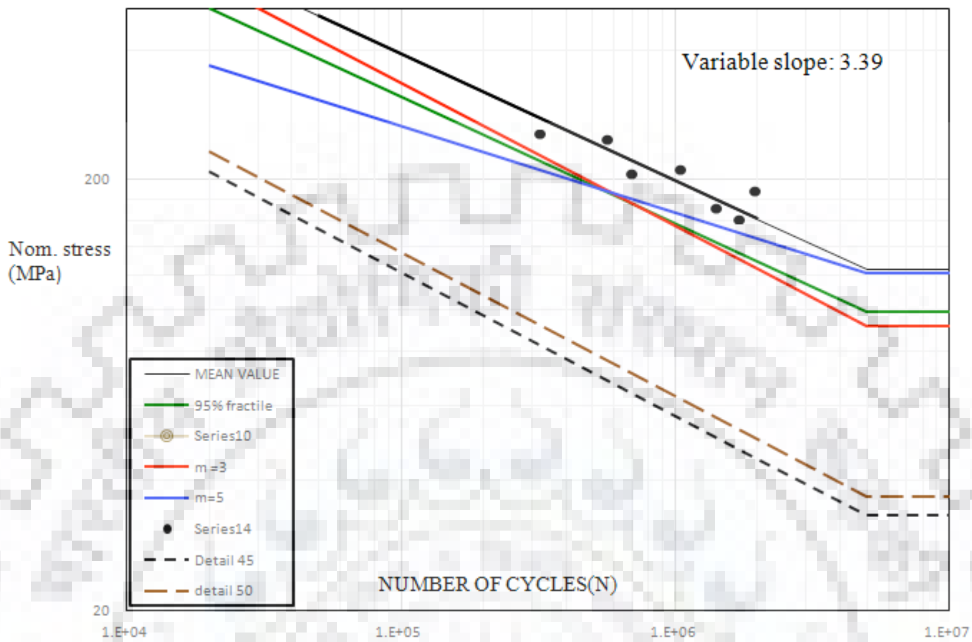

Figure 14. Test results of series 2-4-JSSC 13 without run out shown on logarithmic scale

In the above data, number of test done was 8 and last one was run out marked with an arrow sign. This data was statistically analyzed using prediction interval and following graph was obtained.

Statistical analysis gives a value of 124 MPa for 95% fractile and 157 MPa for 50% fractile for a constant slope m=3 calculated at 2 million cycles. Also, 129 MPa for 95% fractile and 162 MPa for 50% fractile for a variable slope m = 3.39 calculated at 2 million cycles.

4.3.2 Statistical Evaluation of Source 20

Series belonging to source 20 is 3_5_LCW 6. The title of the source is "A re-analysis of fatigue data for welded joints in steel" written by T.R. Gurney. In this source no new test were performed and only re analysis of the existing data is done [20]. Based on the previous analysis new proposals are put forward for revised design stresses. Original sources from detail 5 are 21 and 22. Hence, we do not have any test data to perform statistical analysis.

4.3.3 Statistical Evaluation of source 21

Five series belongs to source ID number 21. These are 6_19, 6_20, 6_21, 6_22, 6_23. Title of the source is "Some fatigue test performed on load carrying fillet welds" by B.S. Macfarlane [21]. The specimens are transversely fillet welded as shown in Fig. 15. Steel grade used for 3 of the series is BS 15 while steel grade for 2 of the series is BS 968 which is considered to be a high strength structural steel.

Table 7: Mechanical properties of steel grade BS15 & BS 968

Steel Grade	Yield stress(MPa)	Tensile stress (MPa)
BS 15	252	450
BS 968	389	617

All tests were carried out under constant amplitude loadings. All the four series with common steel grade differ in the size of the main plate and the cover plate and also the number of run of welding the specimen. Data for all the series was available in tabular form. In case of the weld failure, Crack propagates from the weld root whereas plate failure are said to occur when crack initiates at the weld toe and propagates through the main plate. Rutile Electrode is used to weld all the specimens. Specimens for all the series is T-type transverse fillet welded joint as shown in Fig. 15. Width of the entire specimen is 102 mm. Fatigue test were terminated when there is complete rupture of the specimen either through the fillet weld or through the main plate.

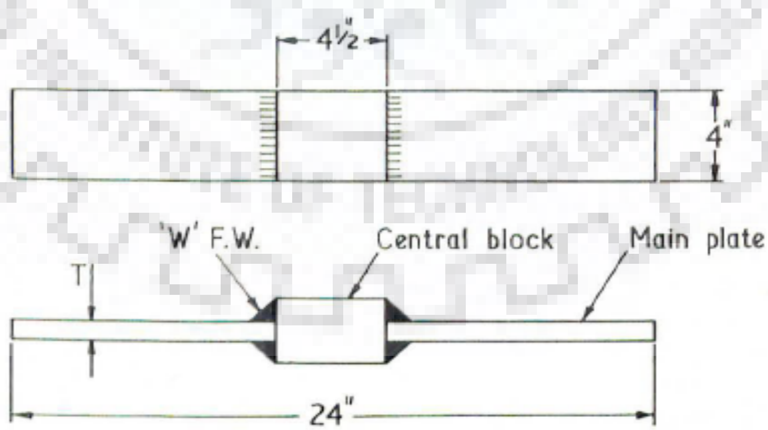

Figure 15. T- type transverse fillet welded joint

1) Statistical results for series 6-19

Series in source is CTN 4. For this series main plate thickness and over plate thickness is 12.7 mm. The tests data was available in tabular form in the source. Steel grade used for this series is BS15. In the available data numbers of test done were 8 and there was one run out. This data was statistically analyzed using prediction interval and following graph was obtained.

Statistical analysis gives a value of 84 MPa for 95% fractile and 103 MPa for 50% fractile for a constant slope m=3 calculated at 2 million cycles. Also, 109 MPa for 95% fractile and 115 MPa for 50% fractile for a variable slope m = 3.86 calculated at 2 million cycles. Crack initiated at the weld toe for all the specimens i.e. Plate failure. Steel grade used for this particular series is BS 15.

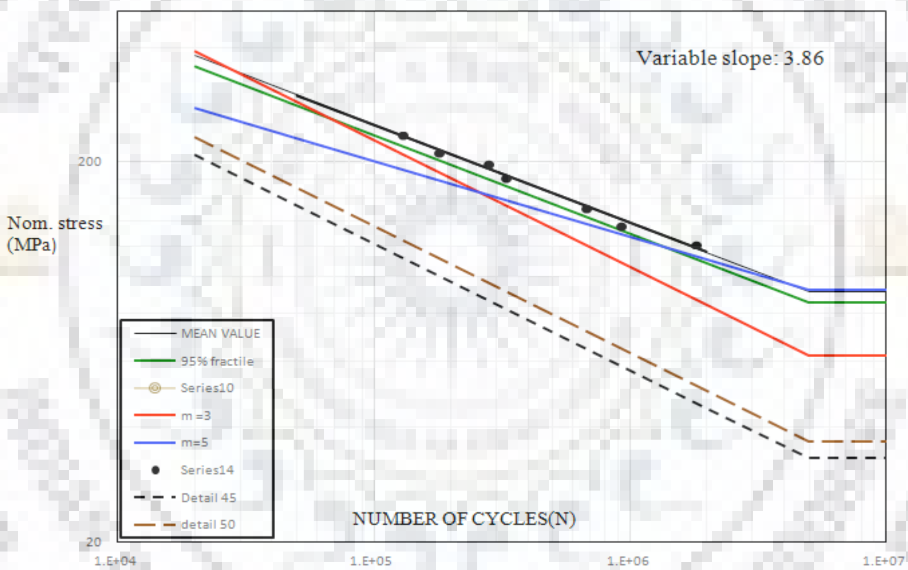

Figure 16. Test results of series 6-19 without run out shown on Logarithmic curve

2) Statistical results of series 6-20

Series in source is CTN 2. For this series main plate thickness is 12.7 mm and over plate thickness is 8 mm. The tests data was available in tabular form in the source. Steel grade used for this series is BS15. In the above data number of test done were 8 and there is no run out i.e. all the specimen failed during the test. This data was statistically analyzed using prediction interval and following graph was obtained. Statistical analysis gives a value of 55 MPa for 95% fractile and 75 MPa for 50% fractile for a constant slope m=3 calculated at 2 million cycles.

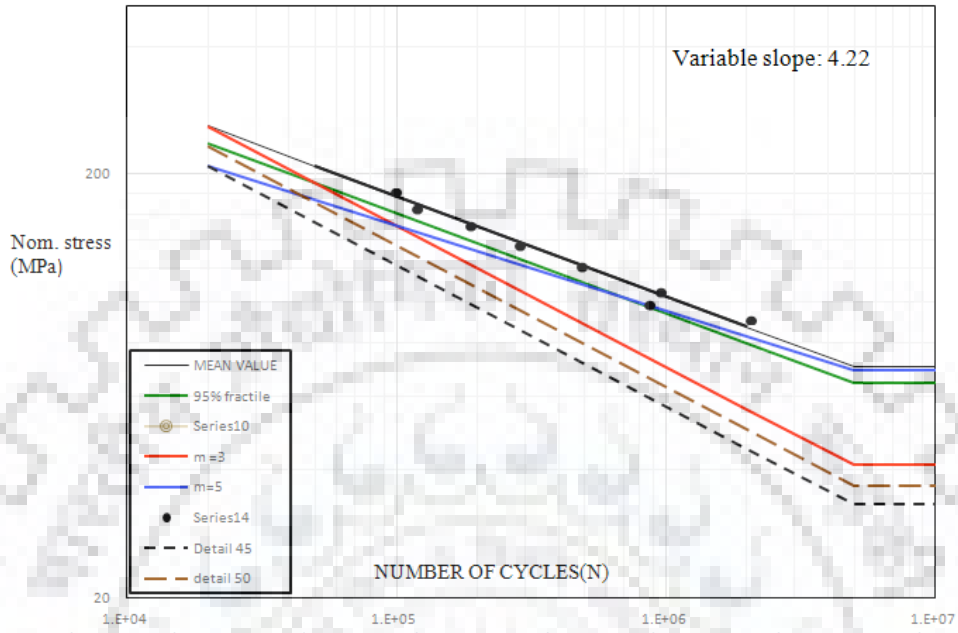

Figure 17. Test results of series 6-20 without run out shown on Logarithmic curve

Also, 80 MPa for 95% fractile and 87 MPa for 50% fractile for a variable slope m = 4.22 calculated at 2 million cycles. Crack initiated at the weld root for maximum of the specimens i.e. weld failure and for only one specimen crack initiated at the weld toe

3) Statistical results of series 6-21

Series in source is CTN 3. The tests data was available in tabular form in the source.

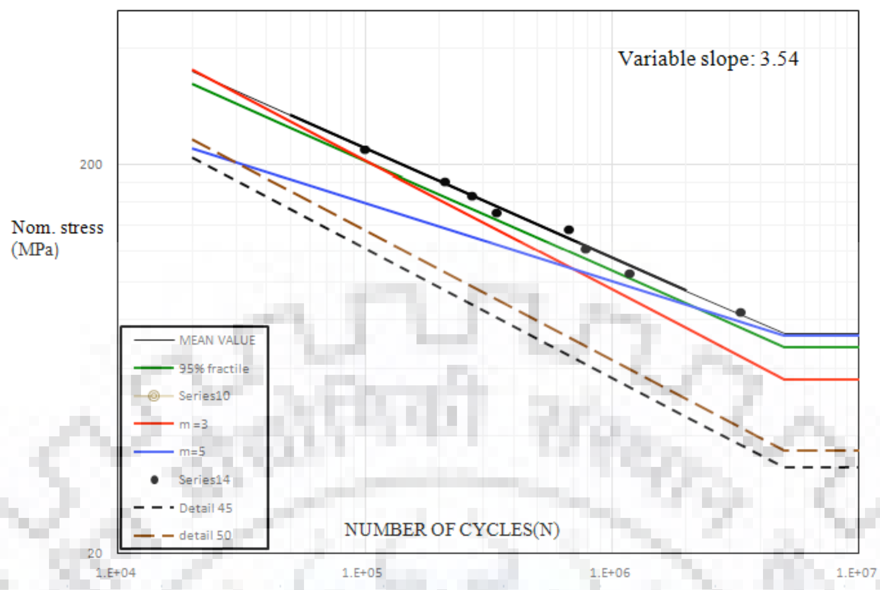

Figure 18. Test results of series 6-21 without run out shown on Logarithmic curve

For this series main plate thickness and over plate thickness is 12.7 mm. Steel grade used for this series is BS 15. In the available data number of test done were 8 and there is no run out i.e. all the specimen failed during the test. This data was statistically analyzed using prediction interval and following graph was obtained. Statistical analysis gives a value of 76 MPa for 95% fractile and 95 MPa for 50% fractile for a constant slope m=3 calculated at 2 million cycles. Also, 88 MPa for 95% fractile and 89 MPa for 50% fractile for a variable slope m = 3.54 calculated at 2 million cycles. In this series half of specimens show failure at weld toe and half of them shows at weld root.

4) Statistical results of series 6-22

Series in source is H CTN 1. For this series main plate thickness and over plate thickness is 8 mm. Steel grade used for this series is BS 968. In the available data number of test done were 8 and there is no run out i.e. all the specimen failed during the test. This data was statistically analyzed using prediction interval and following graph was obtained. The tests data was available in tabular form in the source.

Statistical analysis gives a value of 76 MPa for 95% fractile and 96 MPa for 50% fractile for a constant slope m=3 calculated at 2 million cycles. Also, 95 MPa for 95% fractile and 105 MPa for 50% fractile for a variable slope m = 3.96 calculated at 2 million cycles. In this series all the specimens shows failure at the weld toe i.e. the plate failure.

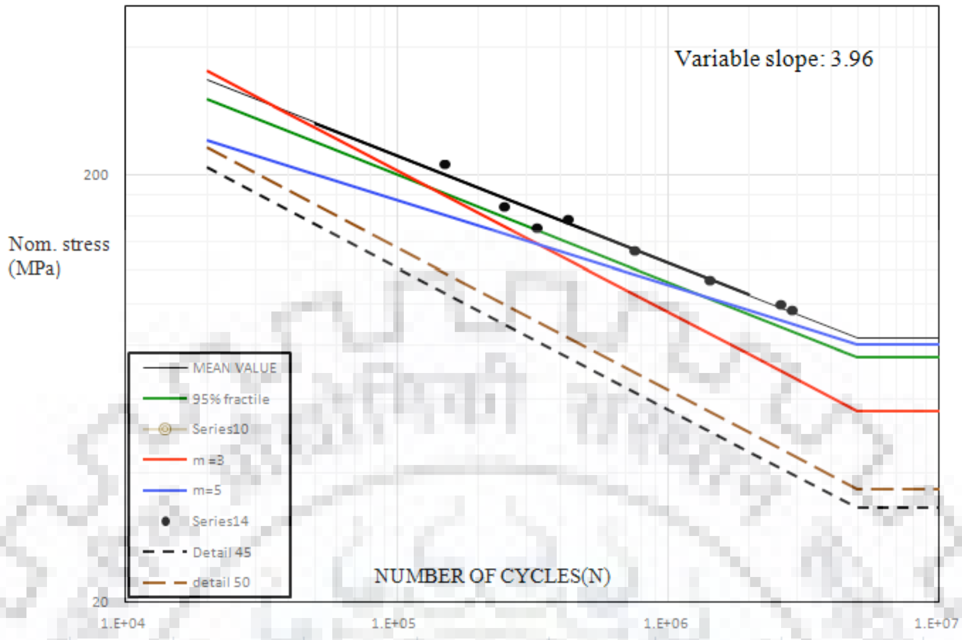

Figure 19. Test results of series 6-22 without run out shown on Logarithmic curve

5) Statistical results of series 6-23

Series in source is H CTN 5. For this series main plate thickness and over plate thickness is 19 mm. Steel grade used for this series is BS 968. In the available data, number of test done were 7 and there is no run out i.e. all the specimen failed during the test. This data was statistically analyzed using prediction interval and following graph was obtained.

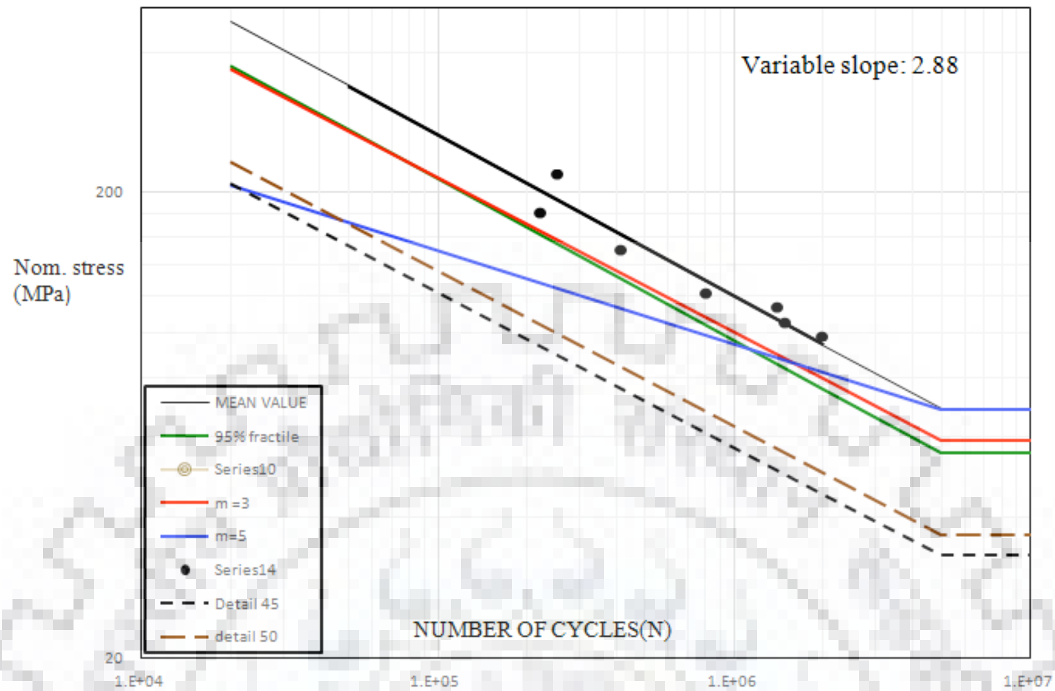

Figure 20. Test results of series 6-23 without run out shown on Logarithmic curve

Statistical analysis gives a value of 80 MPa for 95% fractile and 96 MPa for 50% fractile for a constant slope m=3 calculated at 2 million cycles. Also, 76 MPa for 95% fractile and 94 MPa for 50% fractile for a variable slope m = 2.88 calculated at 2 million cycles. In this series 6 specimen's shows failure at the weld toe i.e. the plate failure, while one specimen shows weld failure.

4.3.4 Statistical evaluation of source 133

Three series belongs to source ID number 133. These are 6_27, 6_28, 6_29. Title of the source is "The comparison of the fatigue strength of welded joints in Structural Steel made at Sheffield University and Military Engineering Experimental Establishment" [21]. The source was not available at the university.

4.3.5 Statistical evaluation of source 22

15 series belongs to source ID number 22. These are 6_32; 6_33; 6_34; 6_35; 6_36; 6_37; 6_38; 6_39; 6_40; 6_41; 6_42; 6_43; 6_44; 6_45; 6_46. Title of the source is" Some factors affecting the fatigue strength of fillet welds" by D. E. Baxter and G. F. Modlen. Specimens are made up of mild steel. Not much information about the composition of the steel is given in the source. The standard specimens with width 38 mm were tested in a 35 tonne Losenhausen machine with a minimum load of 1 tonne and specimens with width 5.1 mm were tested in a 6 tonne Losenhausen machine. Specimens with width 1.3 mm were tested in a 272 kg Avery Schenck pulsator [22]. All the series are divided into different categories depending upon the width of the specimen, type of electrode used for welding, number of weld runs, amount of sulphur content, etc..

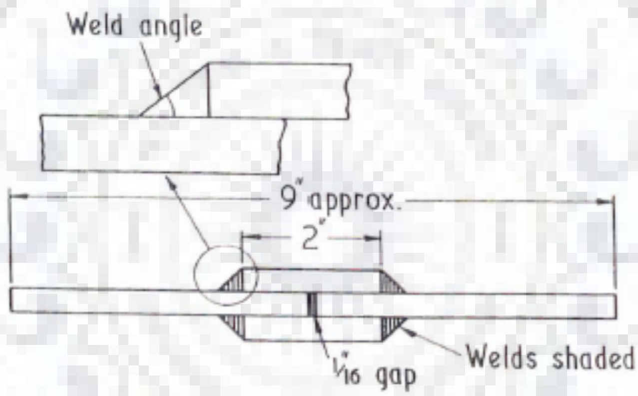

Figure 21. Specimen details of the above series

Four types of electrodes are used to weld the specimen for this source. Details of electrodes are given in table below.

Table 6: Details of electrode used

Electrode	BS. 1719 Code	Remarks
A	E 616	Low hydrogen lime–fluorspar coating; weld metal approx. 35 tons/sq.in. U.T.S.
B	E 917	Iron powder–rutile type; low hydrogen deposit
C	E 619	Low hydrogen lime–fluorspar coating; weld metal approx. 55 tons/sq.in. U.T.S.
D	E 916	Iron and powder coating, giving high deposition rates and deep penetration.

Three different specimens width are considered. These are 38 mm, 5.1 mm, 1.3 mm. All the three specimens are welded with two different electrodes i.e. Electrode A and Electrode B given in table 13. So therefore there are total 6 series that are to be considered. These are: 6_32; 6_33; 6_34; 6_35; 6_36; 6_37.

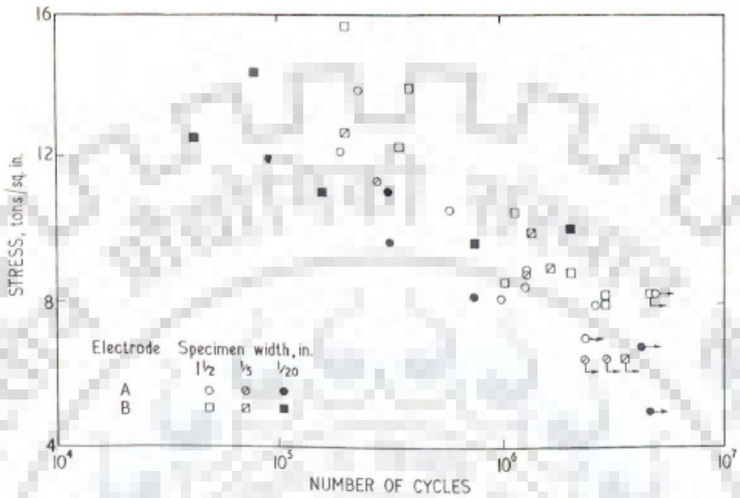

Figure 22. S-N diagram for Mild steel specimens with various thickness and electrodes

1) Statistical evaluation of series 6-32

The width of the specimen is 38 mm and welded with electrode B.

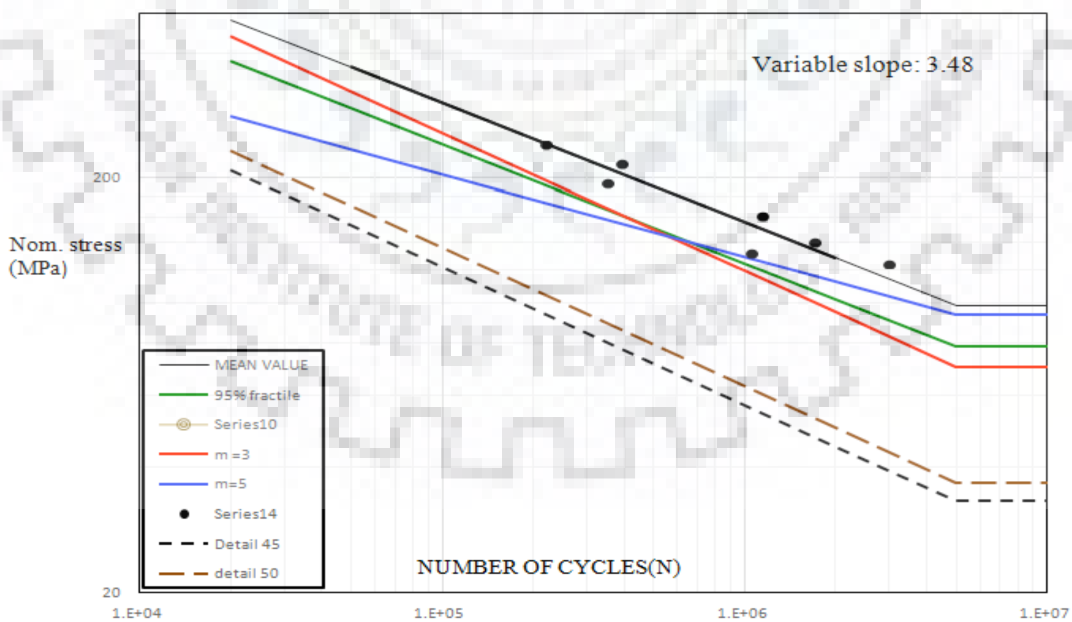

Figure 23. Test results of series 6-32 without run out shown on Logarithmic curve

Data points were extracted from the graph and plotted on S-N curve shown below. Out of 8 specimens one specimen specifies a run out. Failure region of all the specimens is not defined in the source. The test data was statistically analyzed using prediction interval and following graph was obtained. Statistical analysis gives a value of 95 MPa for 95% fractile and 123 MPa for 50% fractile for a constant slope m=3 calculated at 2 million cycles. Also, 102 MPa for 95% fractile and 128 MPa for 50% fractile for a variable slope m = 3.48 calculated at 2 million cycles.

2) Statistical evaluation of series 6-33

The width of the specimen is 38 mm and welded with electrode A. Number of test specimens are 9. Out of which two of the specimens shows a run out which are marked with an arrow sign in the graph. Failure region is not specified for any of the specimen. The test data was statistically analyzed using prediction interval and following graph was obtained.

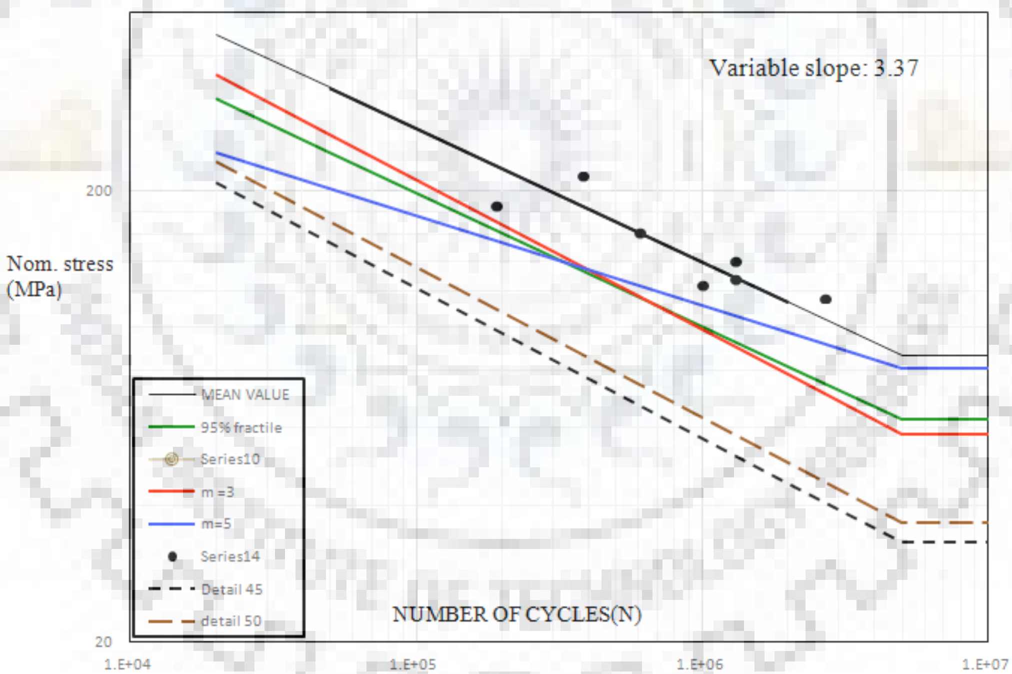

Figure 24. Test results of series 6-33 without run out shown on Logarithmic curve

Statistical analysis gives a value of 78 MPa for 95% fractile and 110 MPa for 50% fractile for a constant slope m=3 calculated at 2 million cycles. Also, 82 MPa for 95% fractile and 114 MPa for 50% fractile for a variable slope m = 3.37 calculated at 2 million cycles.

3) Statistical evaluation of series 6-34

The width of the specimen is 5.1 mm and welded with electrode B. Number of test specimens are 4. Out of which one of the specimen show run out which are marked with an arrow sign. Failure region is not specified for any of the specimen. The test data was statistically analyzed using prediction interval and following graph was obtained.

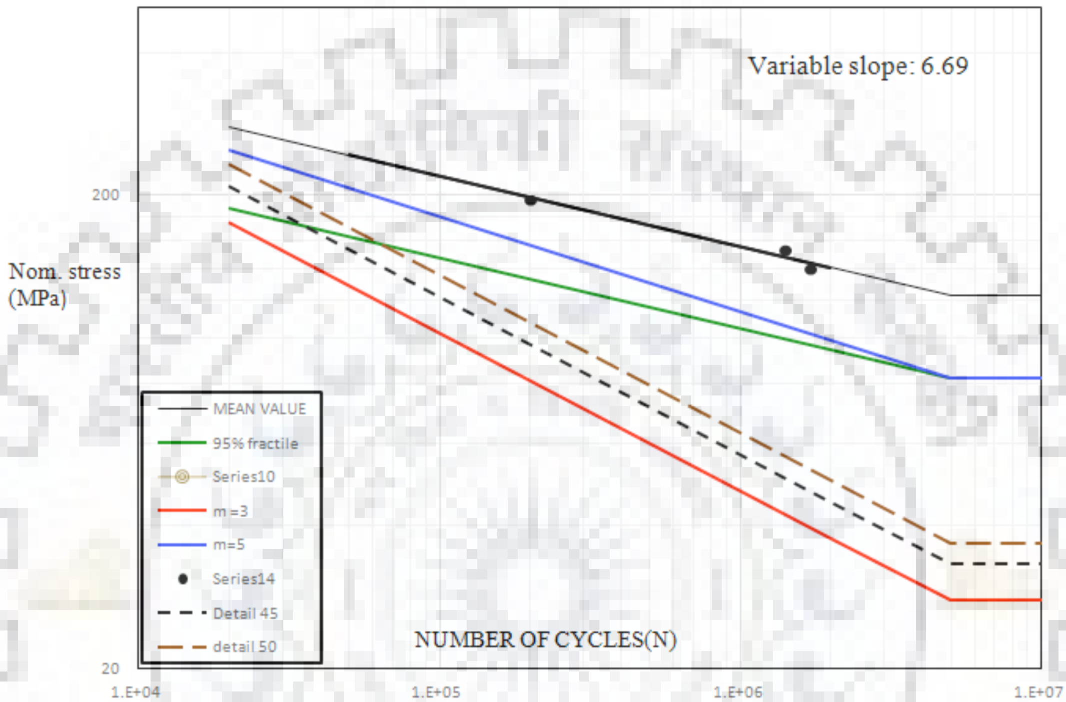

Figure 25. Test results of series 6-34 without run out shown on Logarithmic curve

Statistical analysis gives a value of 38 MPa for 95% fractile and 118 MPa for 50% fractile for a constant slope m=3 calculated at 2 million cycles. Also, 95 MPa for 95% fractile and 140 MPa for 50% fractile for a variable slope m = 6.69 calculated at 2 million cycles. As the number of test specimens are less than 4 the series does not give accurate statistical results.

4) Statistical evaluation of series 6-35

The width of the specimen is 5.1 mm and welded with electrode A. Number of test specimens are 4. Out of which two of the specimens shows a run out which are marked with an * sign. Failure region is not specified for any of the specimen. The test data was statistically analyzed using prediction interval and following graph was obtained. Statistical analysis gives a value of 1.18 MPa for 95% fractile and 104 MPa for 50% fractile for a constant slope m=3 calculated at 2 million cycles. Also 133 MPa for 50%

fractile for a variable slope m = 7.91 calculated at 2 million cycles. As the numbers of test data available for statistical analysis are only 2, the series gives very low value of fatigue strength for 95% fractile and very high value of slope.

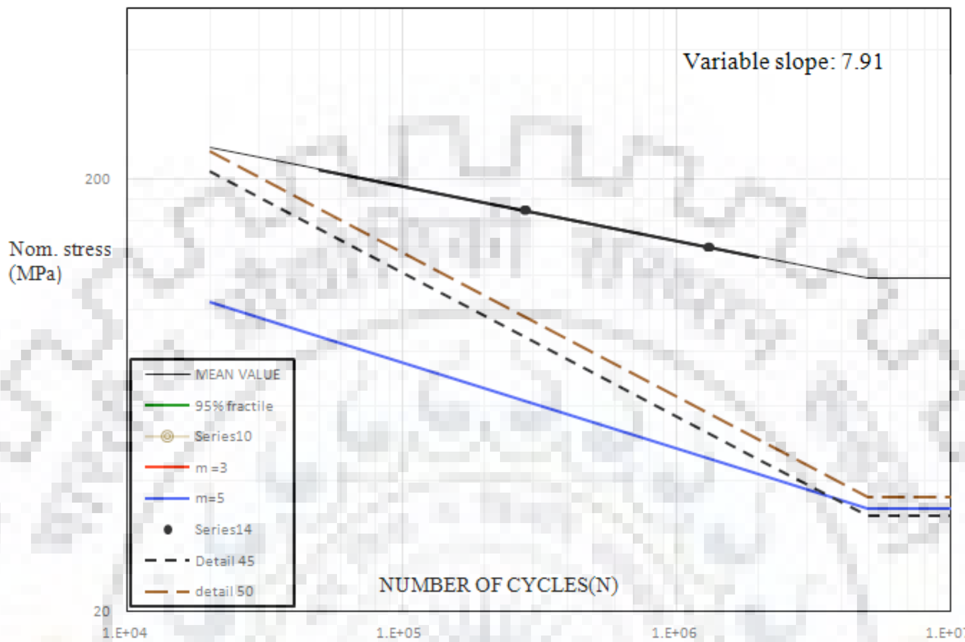

Figure 25. Test results of series 6-35 without run out shown on Logarithmic curve

5) Statistical evaluation of series 6-36

The width of the specimen is 1.3 mm and welded with electrode B. Number of test specimens are 5. No specimen shows a run out. Failure region is not specified for any of the specimen. The test data was statistically analyzed using prediction interval and following graph was obtained.

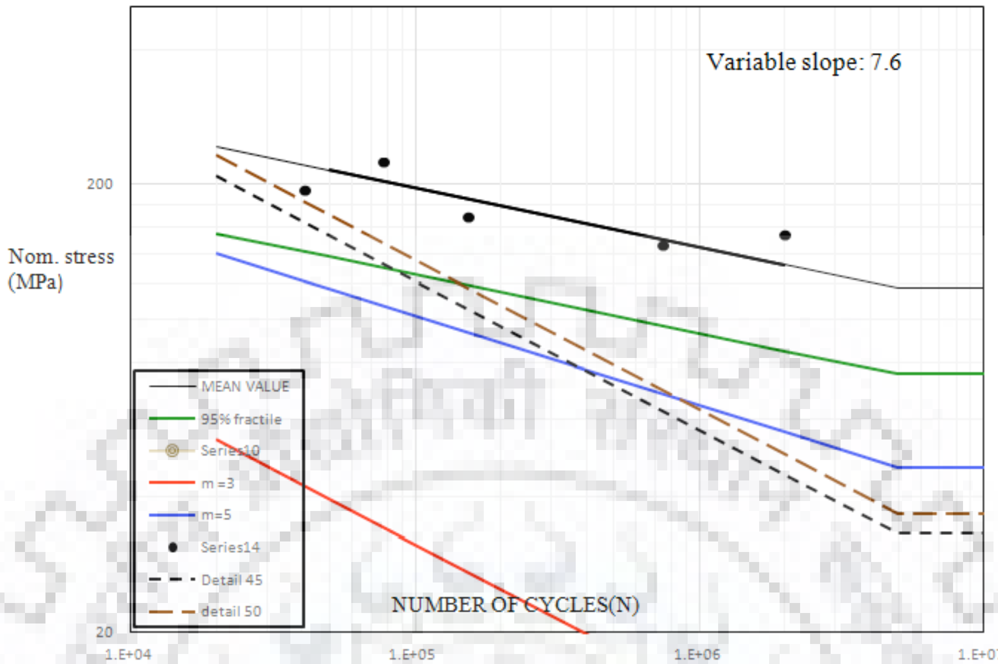

Figure 26. Test results of series 6-36 without run out shown on Logarithmic curve

Statistical analysis gives a value of 11.64 MPa for 95% fractile and 86 MPa for 50% fractile for a constant slope m=3 calculated at 2 million cycles. Also, 85 MPa for 95% fractile and 133 MPa for 50% fractile for a variable slope m = 7.6 calculated at 2 million cycles. As the numbers of test data available for statistical analysis are only 2, the series gives very low value of fatigue strength for 95% fractile and very high value of slope.

6) Statistical evaluation of series 6-37

The width of the specimen is 1.3 mm and welded with electrode A. Number of test specimens are 6. Two of the specimens show a run out and those are marked with an arrow sign. Failure region is not specified for any of the specimen. The test data was statistically analyzed using prediction interval and following graph was obtained.

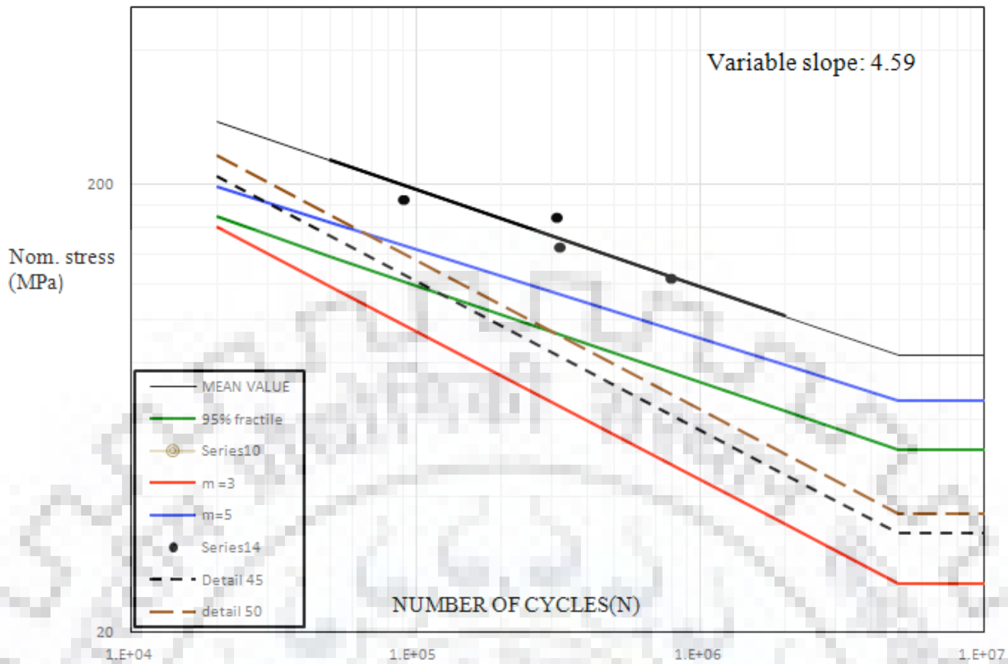

Figure 27a. Test results of series 6-37 without run out shown on Logarithmic curve

Statistical analysis gives a value of 35 MPa for 95% fractile and 82 MPa for 50% fractile for a constant slope m=3 calculated at 2 million cycles. Also, 62 MPa for 95% fractile and 102 MPa for 50% fractile for a variable slope m = 4.59 calculated at 2 million cycles. As the numbers of test data available for statistical analysis are only 4, the series gives very low value of fatigue strength for 95% fractile and very high value of slope.

Researchers thought that the there may lie a difference between the number of weld run so they took some specimens welded with Electrode D and some of the specimens were single welded while some were double welded.

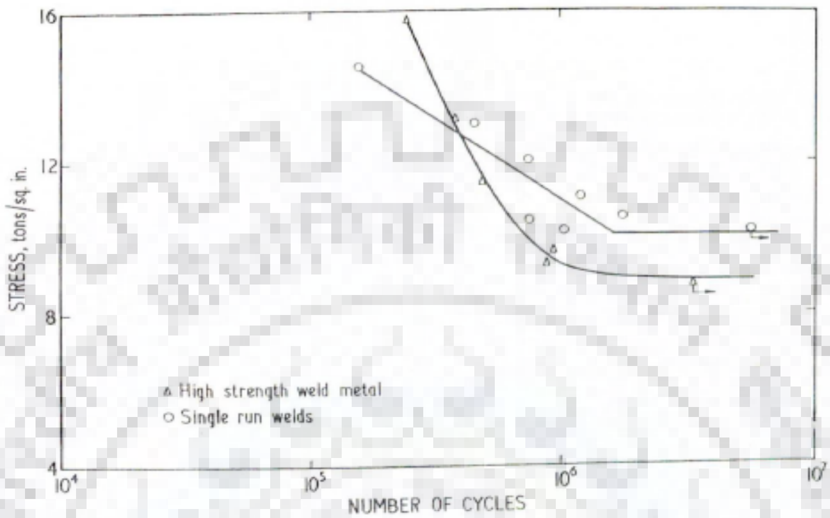

Figure 27b: S-N diagram for Single run specimens and double run specimens

All specimen's have width 1.3 mm. Double weld run Specimens were named as High strength weld metal.

7) Statistical evaluation of series 6-38

Series 6_38 belongs to this type of specimens. Number of test specimens are 8. One of the specimens shows a run out marked with an arrow sign.

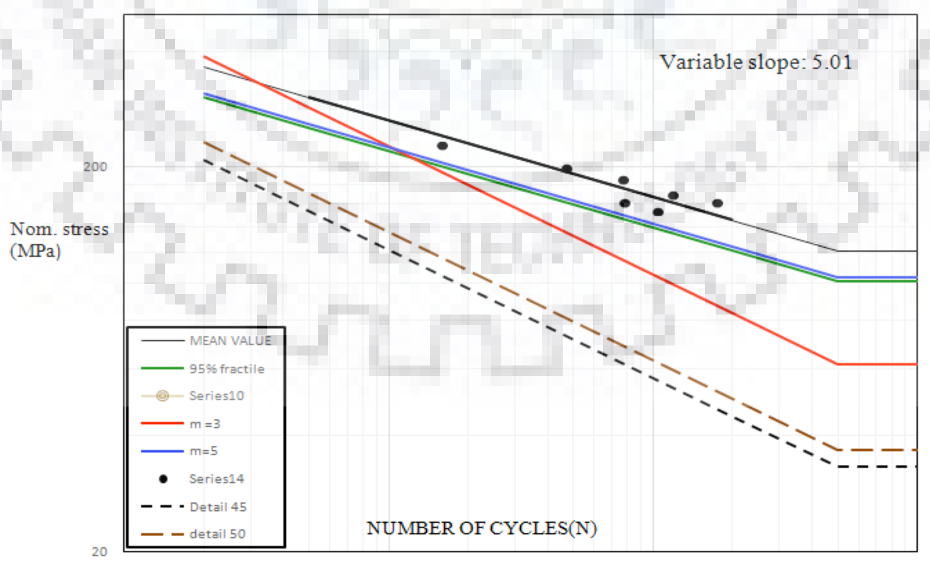

Figure 28. Test results of series 6-38 without run out shown on Logarithmic curve

Failure region is not specified for any of the specimen. The test data was statistically analyzed using prediction interval and following graph was obtained.

Statistical analysis gives a value of 84 MPa for 95% fractile and 127 MPa for 50% fractile for a constant slope m=3 calculated at 2 million cycles. Also, 121 MPa for 95% fractile and 146 MPa for 50% fractile for a variable slope m = 5.01 calculated at 2 million cycles. Series gives very high value of slope.

8) Statistical evaluation of series 6-39

Series 6_39 belongs to this type of specimens. Number of test specimens are 6. One of the specimen shows a run out marked with an arrow sign in Fig. 2.

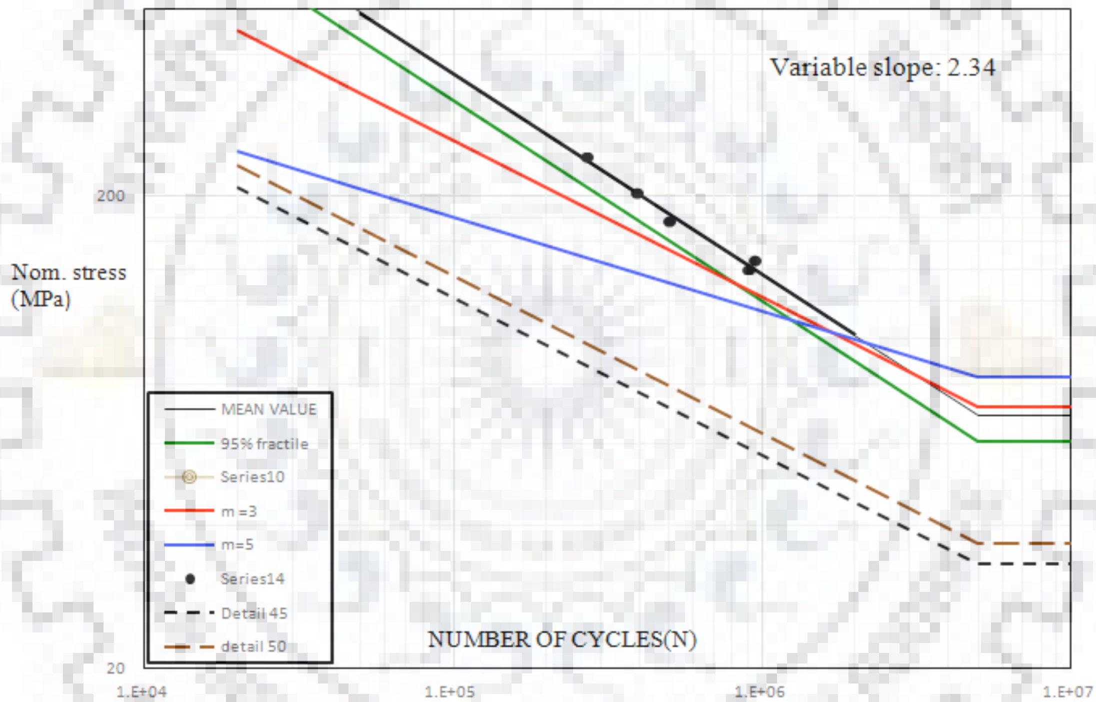

Figure 29. Test results of series 6-39 without run out shown on Logarithmic curve

Failure region is not specified for any of the specimen. The test data was statistically analyzed using prediction interval and following graph was obtained.

Statistical analysis gives a value of 97 MPa for 95% fractile and 115 MPa for 50% fractile for a constant slope m=3 calculated at 2 million cycles. Also, 89 MPa for 95% fractile and 102 MPa for 50% fractile for a variable slope m = 2.54 calculated at 2 million cycles. Series gives low value of slope but high value of fatigue strength for 95% fractile at 2 million cycles.

9) Statistical evaluation of series 6-40

Some specimens were prepared by an inexperienced welders using electrode A. Specimens shows weld defects such as poor root penetration, porosity, undercut and also leg length of the welds was also small. Specimens give low value of fatigue strength than good quality welds.

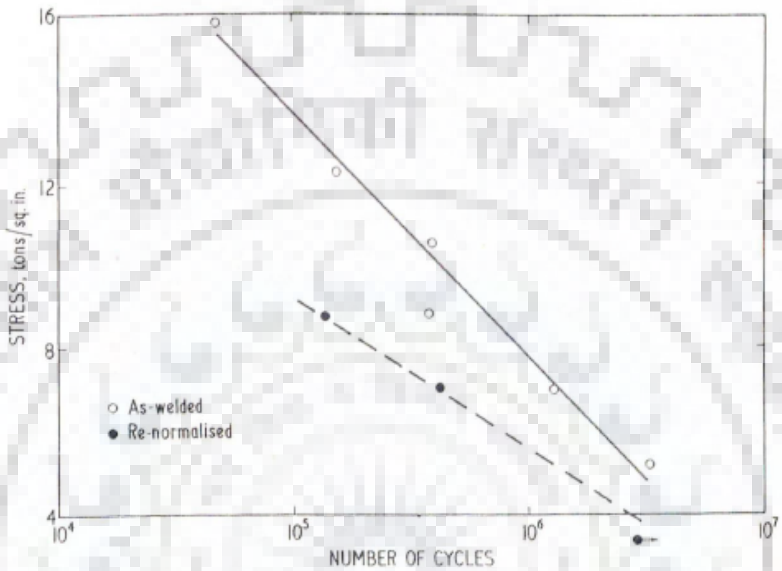

Figure 30. S-N curve for poor quality welds before & after renormalizing

Three of the specimens poorly welded were re- normalized in order to improve fatigue strength by completely removing the residual stresses and elimination of HAZ (Heat affected zone). But the specimens give low value of fatigue strength as decarburization occurs due to re-normalizing.

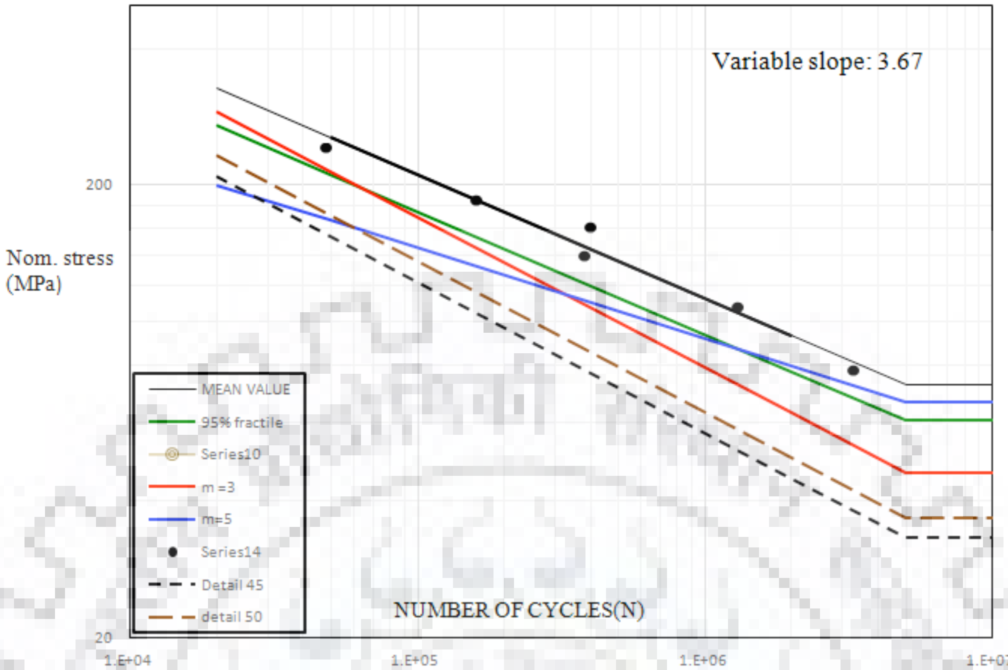

Figure 31. Test results of series 6-40 without run out shown on Logarithmic curve

Poor quality welds gives failure at weld root while the renormalized specimens show failure at weld toe. Series belonging to poor quality weld specimen is 6_40 and renormalized specimens belong to series 6_41. Numbers of specimens tested were 6 and all specimens show failure at weld root. The test data was statistically analyzed using prediction interval and following graph was obtained. Statistical analysis gives a value of 77 MPa for 95% fractile and 85 MPa for 50% fractile for a constant slope m=3 calculated at 2 million cycles. Also, 63 MPa for 95% fractile and 93 MPa for 50% fractile for a variable slope m = 3.67 calculated at 2 million cycles.

10) Statistical evaluation of series 6-41

Only 3 specimens were re normalized and one of the specimen shows a run out marked an * in the given table. Specimen shows failure at weld toe. The test data was statistically analyzed using prediction interval and following graph was obtained.

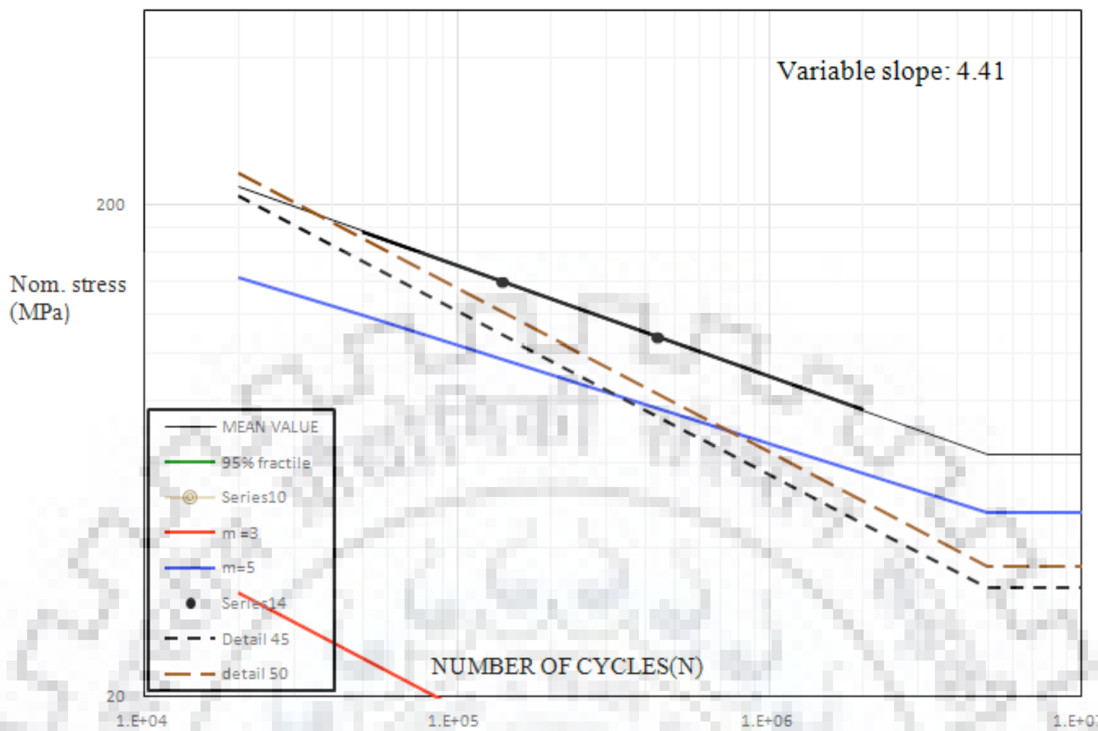

Figure 32. Test results of series 6-41 without run out shown on Logarithmic curve

Statistical analysis gives a value of 6.98 MPa for 95% fractile and 61 MPa for 50% fractile for a constant slope m=3 calculated at 2 million cycles. Also 77 MPa for 50% fractile for a variable slope m = 4.41 calculated at 2 million cycles. As the numbers of test data available for statistical analysis are only 2, the series gives very low value of fatigue strength for 95% fractile and high value of slope.

Research was done to analyze the effect of sulphur content on fatigue strength of high strength steel. Type A electrode was used to weld all the specimens. The study shows that there lies very less difference in fatigue strength of the material by varying the sulphur content.

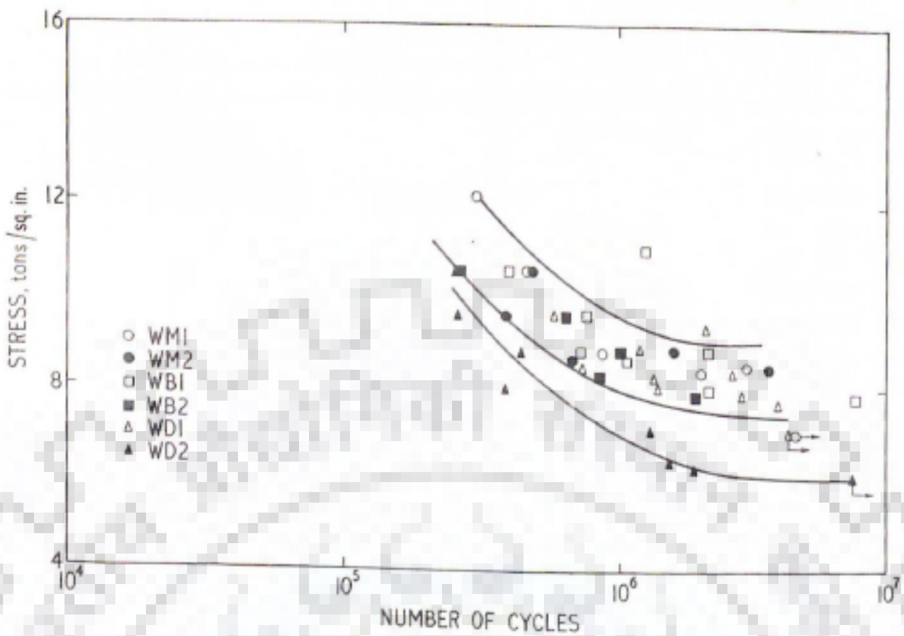

Figure 33. Fatigue test results of welded Specimens with varying sulphur content

Series that belongs under this category are 6_42; 6_43; 6_44; 6_45; 6_46.

11) Statistical evaluation of series 6-42

This Series represents to WM1 in source 91 with a sulphur content of .039%. Test data were collected from S-N curve Fig. 33. Number of test specimens are 6. One of the specimens shows a run out as shown in graph with an arrow sign. Failure region is not specified for any of the specimen. The test data was statistically analyzed using prediction interval and following graph was obtained. Statistical analysis gives a value of 67 MPa for 95% fractile and 113 MPa for 50% fractile for a constant slope m=3 calculated at 2 million cycles. Also, 99 MPa for 95% fractile and 126 MPa for 50% fractile for a variable slope m = 5.29 calculated at 2 million cycles. Series gives high value of slope and fatigue strength for 95% fractile at 2 million cycles.

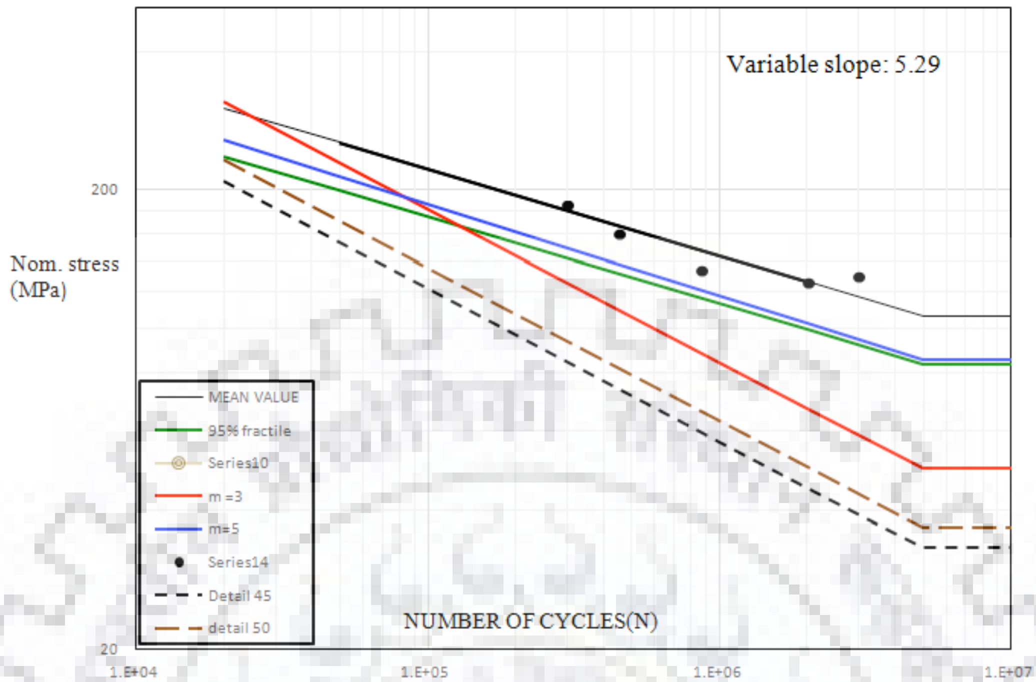

Figure 34. Test results of series 6-42 without run out shown on Logarithmic curve

12) Statistical evaluation of series 6-43

This Series represents to WM2 in source 91 with a sulphur content of .009%. Test data were collected from S-N curve Fig. 33. Number of test specimens are 5. No specimen shows a run out. Failure region was not specified in the source. The test data was statistically analyzed using prediction interval and following graph was obtained.

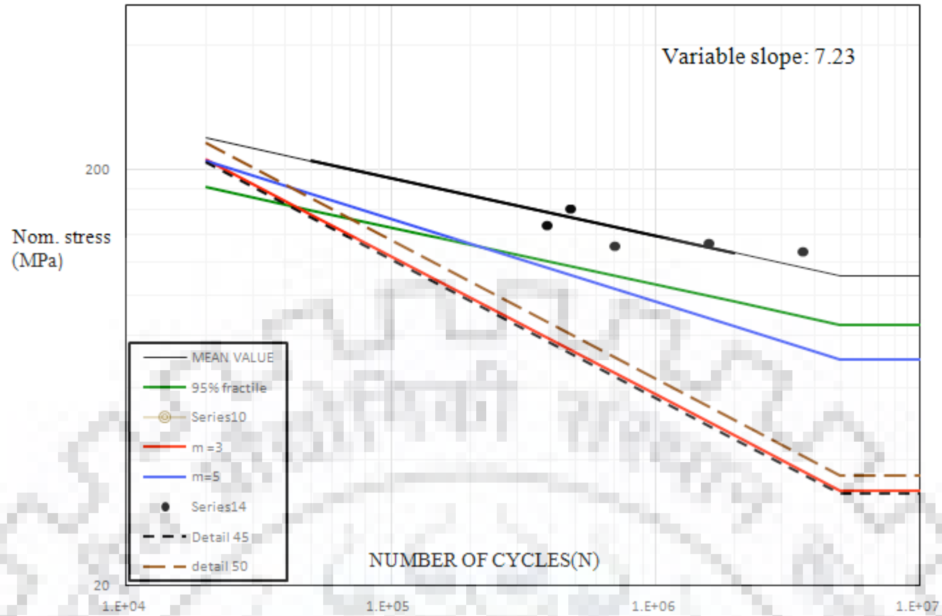

Figure 35. Test results of series 6-43 without run out shown on Logarithmic curve

Statistical analysis gives a value of 46 MPa for 95% fractile and 109 MPa for 50% fractile for a constant slope m=3 calculated at 2 million cycles. Also, 96 MPa for 95% fractile and 126 MPa for 50% fractile for a variable slope m = 7.23 calculated at 2 million cycles. Series gives high value of slope and low value fatigue strength for 95% fractile at 2 million cycles.

13) Statistical evaluation of series 6-44

This Series represents to WB1 in source 91 with a sulphur content of .049%. Test data was collected from S-N curve Fig. 33. Number of test specimens are 8. No specimen shows a run out. Failure region was not specified in the source. The test data was statistically analyzed using prediction interval and following graph was obtained. Test data are available in table below.

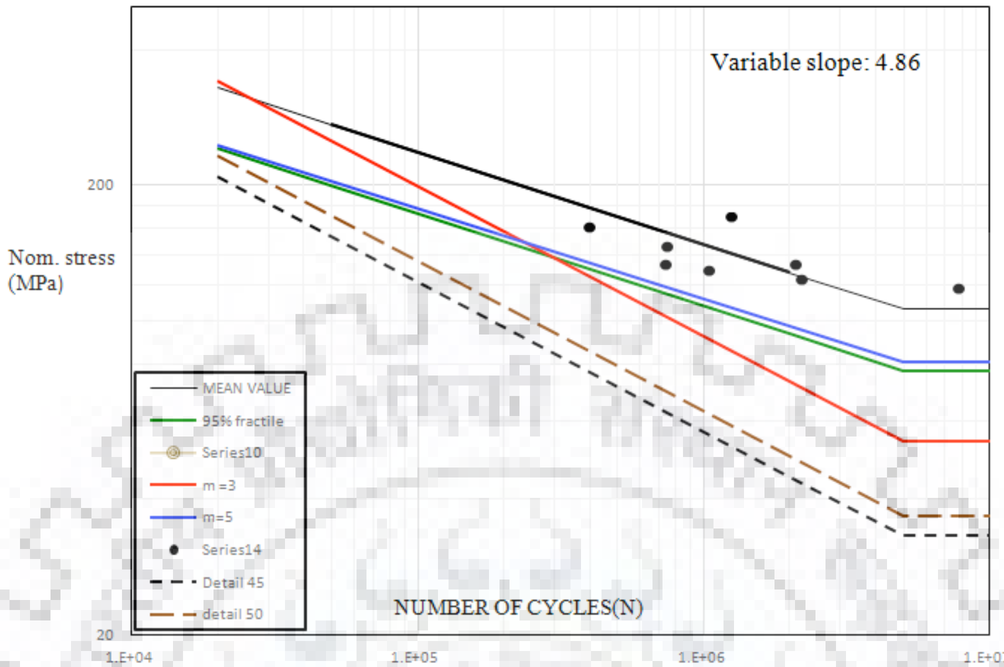

Figure 36. Test results of series 6-44 without run out shown on Logarithmic curve

Statistical analysis gives a value of 73 MPa for 95% fractile and 121 MPa for 50% fractile for a constant slope m=3 calculated at 2 million cycles. Also, 94 MPa for 95% fractile and 128 MPa for 50% fractile for a variable slope m = 4.86 calculated at 2 million cycles. Series gives high value of slope and low value fatigue strength for 95% fractile at 2 million cycles.

14) Statistical evaluation of series 6-45

This Series represents to WB2 & WD2 in source 91 with a sulphur content of .005%. Test data was collected from S-N curve Fig. 33. Number of test specimens are 13. One of the specimens shows a run out. Failure region was not specified. The test data was statistically analyzed using prediction interval and following graph was obtained. In this series 2 specimens with same amount of sulphur are combined.

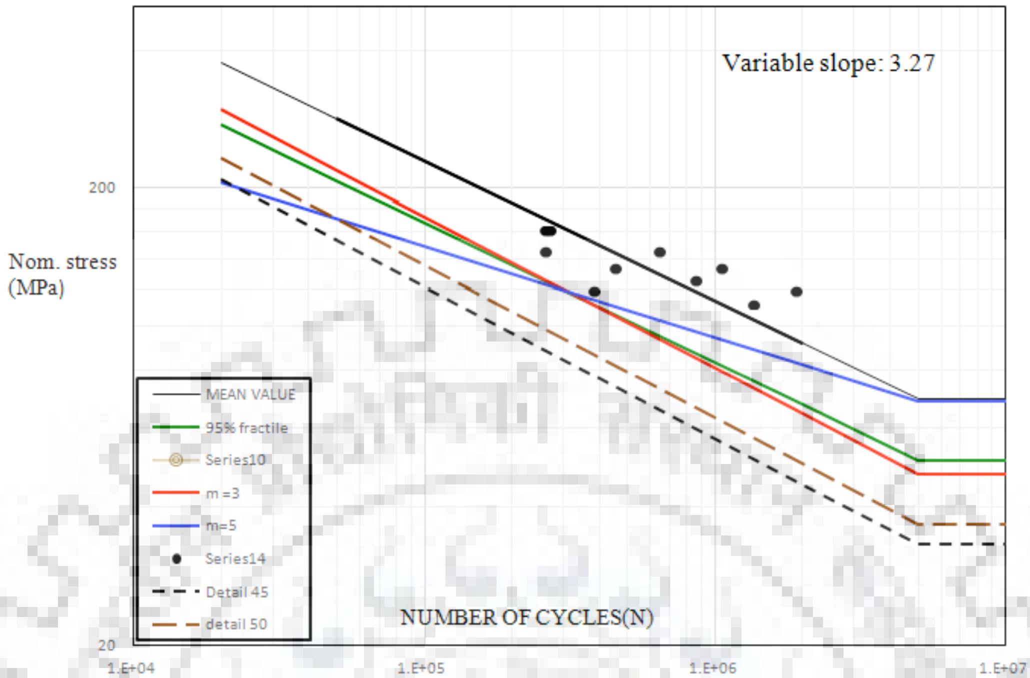

Figure 37. Test results of series 6-45 without run out shown on Logarithmic curve

Statistical analysis gives a value of 64 MPa for 95% fractile and 89 MPa for 50% fractile for a constant slope m=3 calculated at 2 million cycles. Also, 67 MPa for 95% fractile and 92 MPa for 50% fractile for a variable slope m = 3.27 calculated at 2 million cycles. Series give good accurate results due to large number of test data available.

15) Statistical evaluation of series 6-46

This Series represents to WD1 in source 91 with a sulphur content of .043%. Test data was collected from S-N curve Fig. 33. Number of test specimens are 10. One of the specimens shows a run out. Failure region was not specified. The test data was statistically analyzed using prediction interval and following graph was obtained.

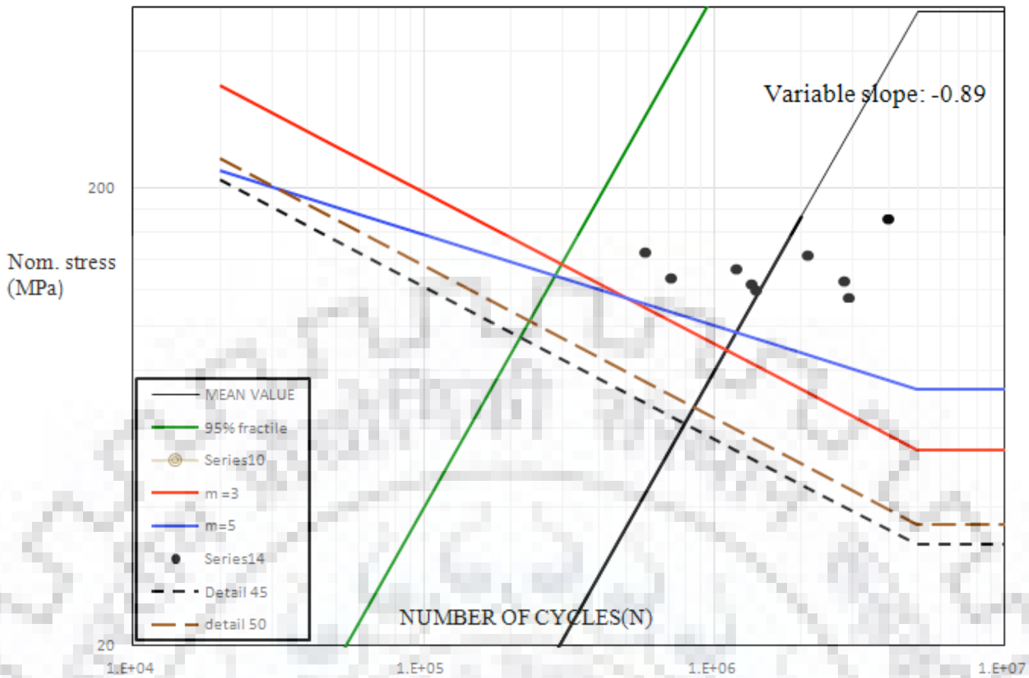

Figure 38. Test results of series 6-46 without run out shown on Logarithmic curve

Statistical analysis gives a value of 73 MPa for 95% fractile and 124 MPa for 50% fractile for a constant slope m=3 calculated at 2 million cycles. Also, 1168 MPa for 95% fractile and 174 MPa for 50% fractile for a variable slope m = -0.89 calculated at 2 million cycles. Data given for this series is not relevant and the slope value is in negative, unable to get statistical results. We can observe in the S-N curve that number of cycles to failure increases with increase in stress range. So with the results, we can conclude that the data given is not relevant.

After obtaining the statistical results of all the series from source 91 we may conclude that all the series are bad as the value of fatigue strength obtained was below the fatigue strength defined in the Eurocode 3.1-9 for detail 5.

Also for source 113, 4 of the series show good statistical results and have higher fatigue strength value than that specified I Eurocode 3.1-9 for detail 5. Series from source 12 also gives good statistical results.

4.3.6 Statistical evaluation of source 23

2 series belongs to source ID number 23. These are: 6_54; 6_55. Title of the source is "Effect of shot peening on the fatigue properties of maraging steel and Al-Zn-Mg alloy". For improving the fatigue life of the welds 3 methods are generally used. These are:

i. Exclusion of atmosphere by rubber and plastic coatings.
ii. Improving profile by grinding.
iii. Introducing residual stress pattern.

Among this introducing residual stresses are generally preferred. This can be achieved thermally or by applying loads. Thermal effects in strong alloys is limited, therefore shot peening method is often used to improve fatigue performance of the structure [23].

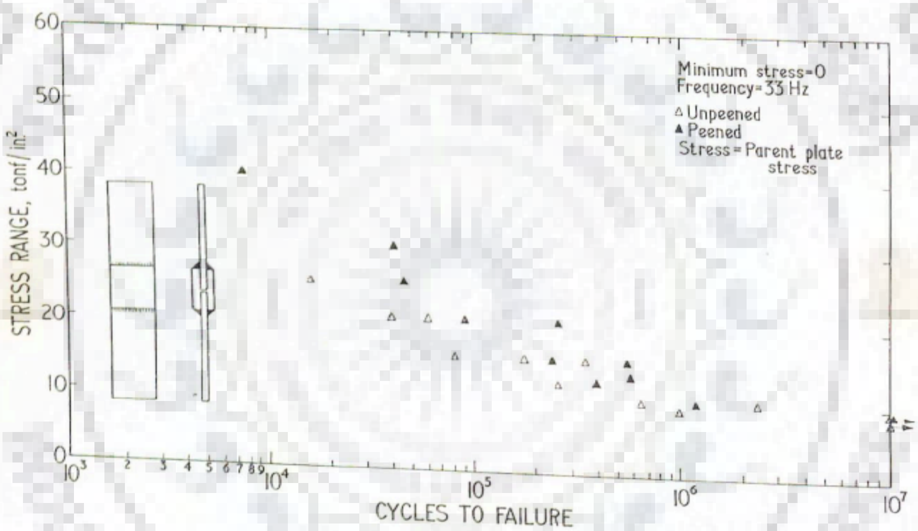

Figure 39. Peened and unpeened transverse load carrying fillet weld specimen

Data from Fig. 39 was extracted and plotted on a S-N curve to know the statistical results for 95% survival probability at 2 million cycles. First S-N curve shows the results of unpeened specimens made up of maraging steel. MIG process is used for welding. 11 specimens were tested and one specimen shows a run out while others show the failure of the parent plate. Series for the unpeened specimen is 6_54.

Statistical analysis gives a value of 59 MPa for 95% fractile and102 MPa for 50% fractile for a constant slope m=3 calculated at 2 million cycles. Also, 93 MPa for 95% fractile and 127 MPa for 50% fractile for a variable slope m = 4.18 calculated at 2 million cycles

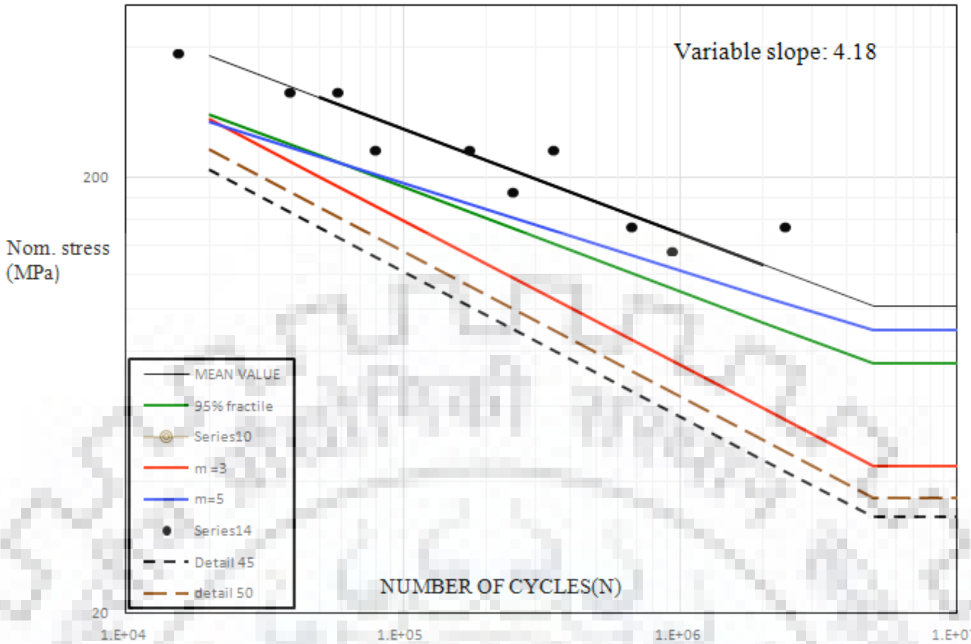

Figure 40. S-N curve for unpeened specimens belonging to series 6-54

Series for peened specimens is 6_55. Total 13 specimens were tested and 2 of the specimens show run out. Specimens were peened using a wheelabrator running at 2250 rev. /min.

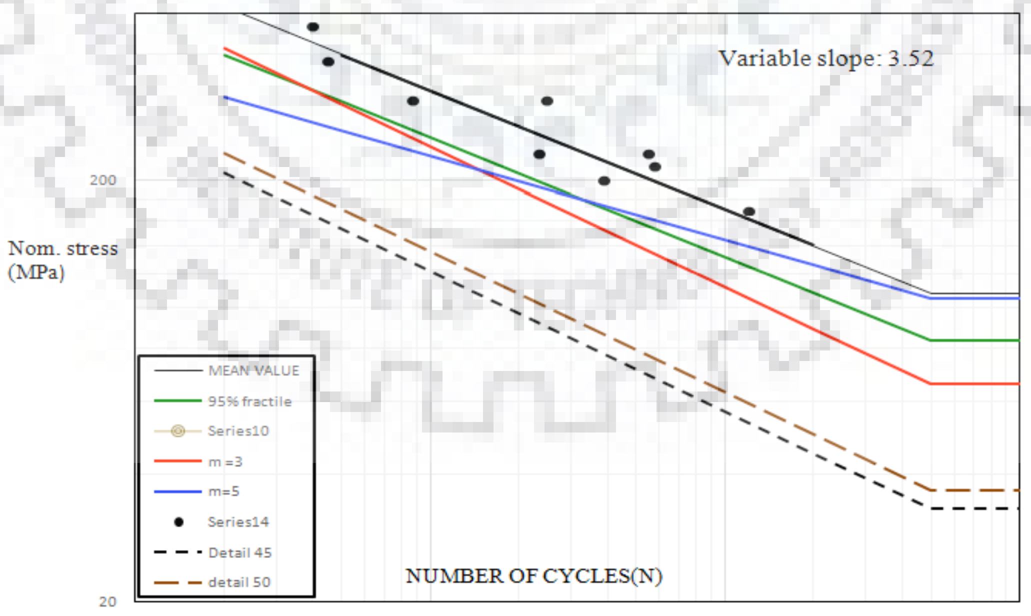

Figure 41. S-N curve for unpeened specimens belonging to series 6-55

Data points from Fig. 39 were taken and were statistically analyzed using prediction interval and following graph was obtained.

Statistical analysis gives a value of 89 MPa for 95% fractile and108 MPa for 50% fractile for a constant slope m=3 calculated at 2 million cycles. Also, 124 MPa for 95% fractile and 140 MPa for 50% fractile for a variable slope m = 3.52 calculated at 2 million cycles.

Peened specimens show an increase in the fatigue strength by 30 MPa for 95 % survival probability for constant slope at 2 million cycles. Both series show good statistical results with high value of fatigue strength.

Hence, we may conclude that total 7 series from detail 5 can be used for further analysis.

In detail 5, there is a controversy with the geometry of the specimens. In Eurocode 3.1-9 table 8.5 only one of specimen is listed which is same as shown in Fig. 13 and other specimen geometry as shown in Fig. 15 is not present in table 8.5. We tried to evaluate series of detail 5 as detail 1 which is a cruciform joint but that also has a complete different geometry. In IIW we found that there are 2 details as shown in Fig. 42 & Fig. 43 below.

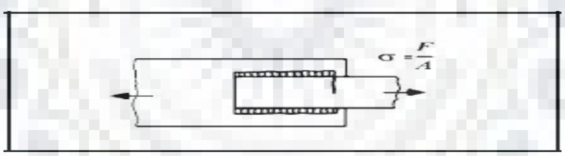

Figure 42a. Longitudinally loaded lapped joint with fillet welds given in IIW having FAT 63

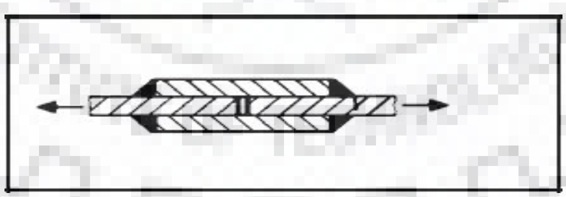

Figure 42b. Transversely loaded lapped joint with side fillet welds given in IIW having FAT 50.

With this we conclude that one more detail with transversely loaded lapped joint should be added in table 8.5 with a value of fatigue strength more than or equal to 50 N/mm^2.

4.4 Evaluation of detail 6

Statistical evaluation results for detail 6 are given below. There are total 25 series and 5 sources available for the evaluation.

4.4.1 Statistical evaluation of source 24

Series belonging to this source is 3_4_NLC 13. The source was available in French language so was not able to extract much information. Two attachments are welded on each flange of Length 50 mm.

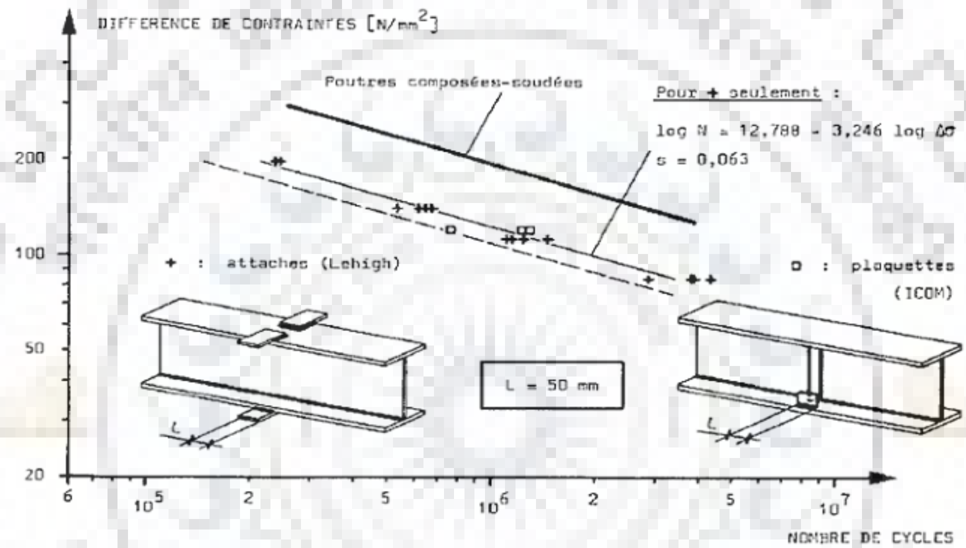

Figure 43a. Data points for series 3-4-NLC 13[24]

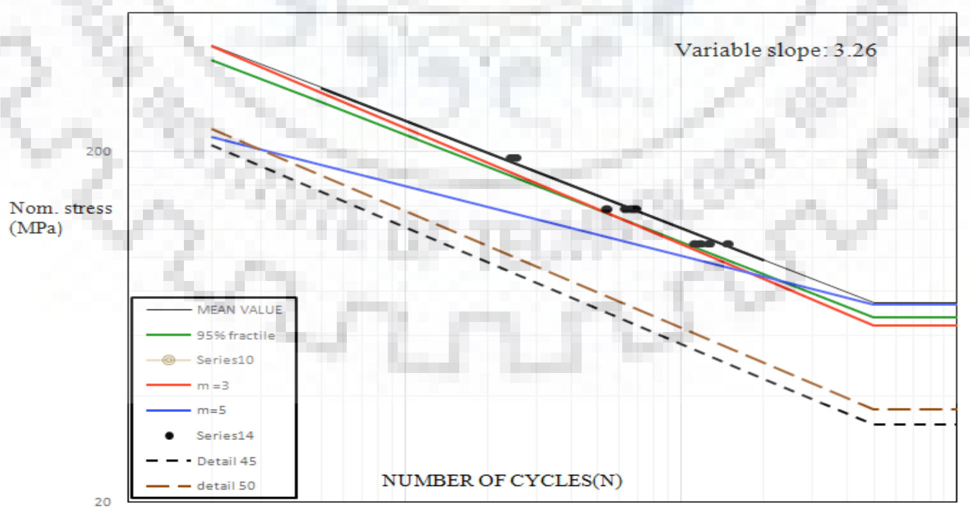

Figure 43b. Test results of series 3_4_NLC 13 without run out shown on Logarithmic curve

Data points from Fig. 42 were taken and were statistically analyzed using prediction interval and following graph was obtained. Statistical analysis gives a value of 87 MPa for 95% fractile and 97 MPa for 50% fractile for a constant slope m=3 calculated at 2 million cycles. Also, 89 MPa for 95% fractile and 98 MPa for 50% fractile for a variable slope m = 3.26 calculated at 2 million cycles.

4.4.2 Statistical evaluation of source 20

Series belonging to source 20 are 3_5_LCW 1; 3_5_LCW 2; 3_5_LCW 3. The title of the source is "A re-analysis of fatigue data for welded joints in steel" written by T.R. Gurney. In this source no new test were performed and only re analysis of the existing data is done [20]. Based on the previous analysis new proposals are put forward for revised design stresses. Original sources for series 3_5_LCW 1 is source 28 series 3_5_LCW 17a; for series 3_5_LCW 2 original source is 28 series 3_5_LCW 18 and for series 3_5_LCW 3 original source is 28 series 3_5_LCW 13.

4.4.3 Statistical evaluation of source 25

Series belonging to source ID number 25 are: 3_5_LCW 15; 3_5_LCW 16; 3_5_LCW 22. In this research data available was tested for variable amplitude loadings [25]. In EC 3.1-9 we are only dealing with constant amplitude loadings for statistical analysis. Hence the statistical analysis for these 3 series was not done.

4.4.4 Statistical evaluation of source 26

Total 8 series belongs to source ID number 26. These are 3_4_NLC 22; 3_4_NLC 23; 3_4_NLC 24; 3_4_NLC 25; 7_137; 7_138; 7_139; 7_140. Geometry of the specimen for this source is shown in Fig. 44. Two cover plates are attached on each flange and length of the attachments

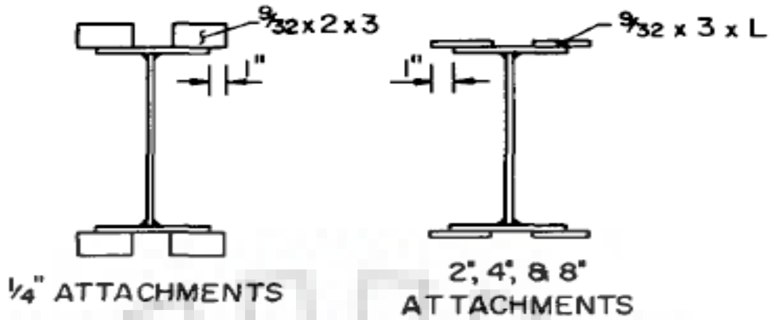

Figure 44. Beams details with Flange attachments

Among 8 series the last four series are the repetition of first 4 series, the only difference is the name of the series, so the evaluation being done for only 4 of the series i.e. 3_4_NLC 22; 3_4_NLC 23; 3_4_NLC 24; 3_4_NLC 25. The difference among these series lies in the length of the attachment as 7.1 mm, 51 mm, 102 mm, and 204 mm. Test data is given in both graphical form as well as tabular form.

1. **Statistical results for series 3-4-NLC 22**

Length of the attachment is 7.1 mm, width of the attachment is 51 mm and thickness of the attachment is 76 mm.

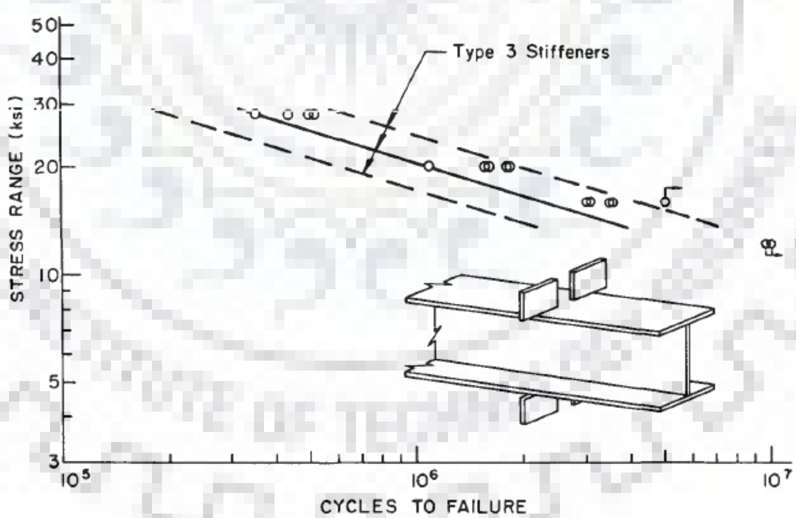

Figure 45. S-N curve for 7.1 mm attachments

Data points were collected from Fig. 45 and were statistically analyzed using prediction interval and following graph was obtained.

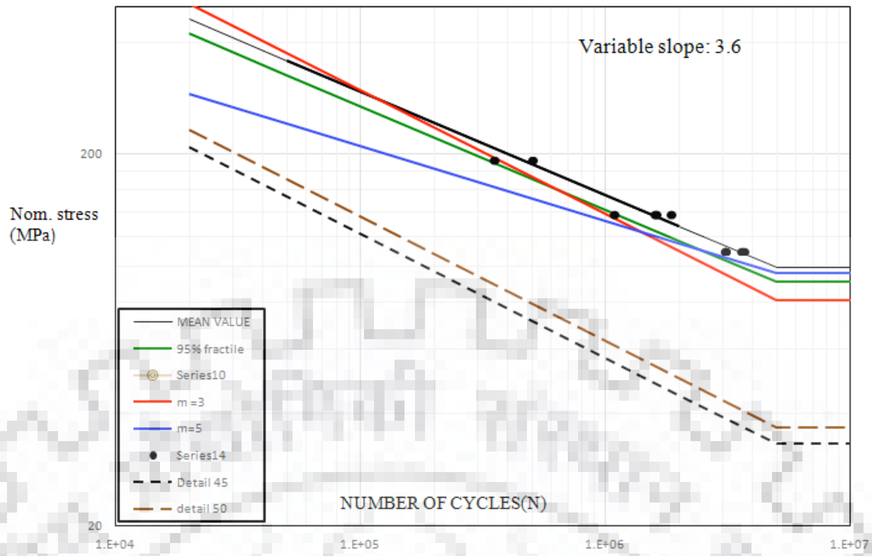

Figure 46. Test results of series 3_4_NLC 22 without run out shown on Logarithmic curve

Statistical analysis gives a value of 110 MPa for 95% fractile and 117 MPa for 50% fractile for a constant slope m=3 calculated at 2 million cycles. Also, 125 MPa for 95% fractile and 128 MPa for 50% fractile for a variable slope m = 3.6 calculated at 2 million cycles.

2. **Statistical evaluation of series 3-4-NLC 23**

Length of the attachment is 51 mm, width of the attachment is 76 mm and thickness of the attachment is 7.2 mm.

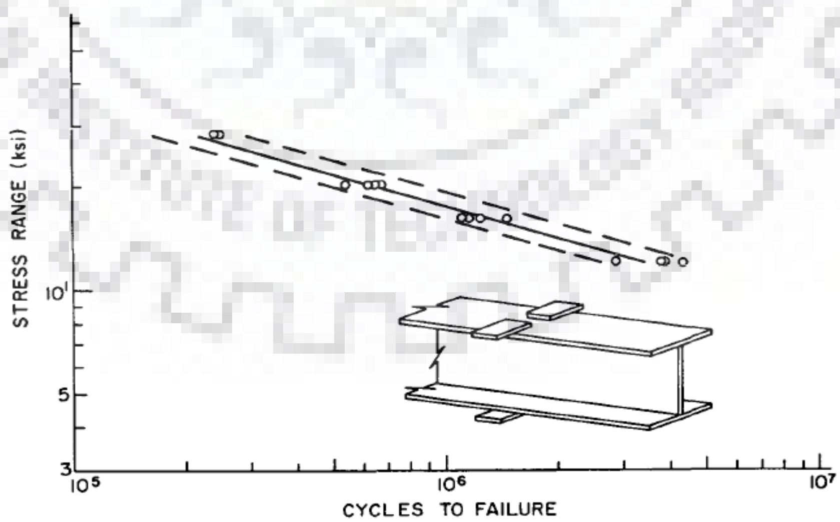

Figure 47: S-N curve for 51 mm attachments

Data points were collected from Fig. 47 and were statistically analyzed using prediction interval and following graph was obtained.

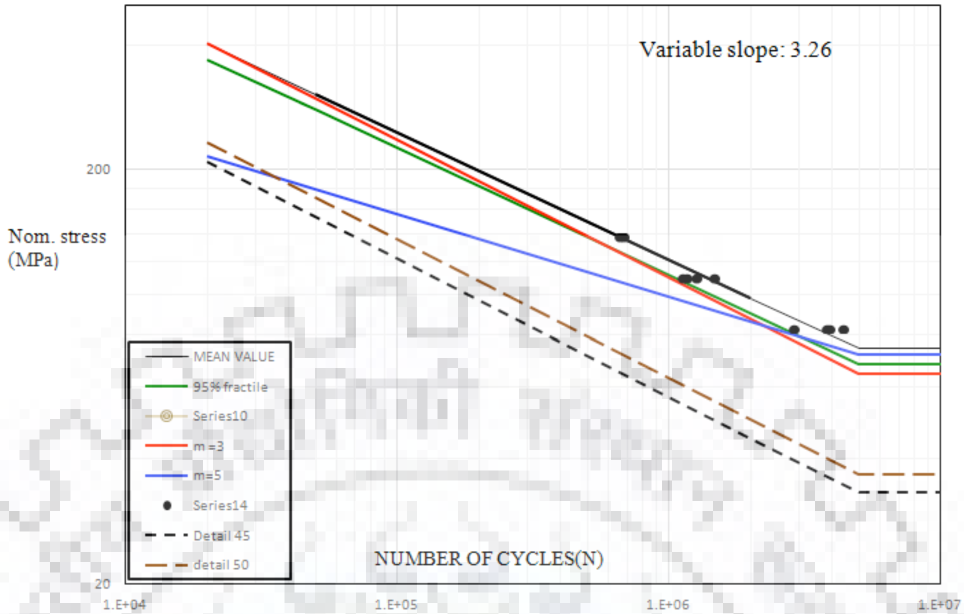

Figure 48 Test results of series 3_4_NLC 23 without run out shown on Logarithmic curve

Fig. 48 shows the statistical result of series 3_4_NLC 23. Statistical analysis gives a value of 87 MPa for 95% fractile and 96 MPa for 50% fractile for a constant slope m=3 calculated at 2 million cycles. Also, 90 MPa for 95% fractile and 98 MPa for 50% fractile for a variable slope m = 3.26 calculated at 2 million cycles.

3. **Statistical evaluation of series 3-4-NLC 24**

Length of the attachment is 102 mm, width of the attachment is 76 mm and thickness of the attachment is 7.2 mm. For this series specimens were divided into 2 sub-series.

i. Specimens only welded longitudinally.

ii. Specimens welded all around.

Data points from two S-N curves was collected and the analyzed.

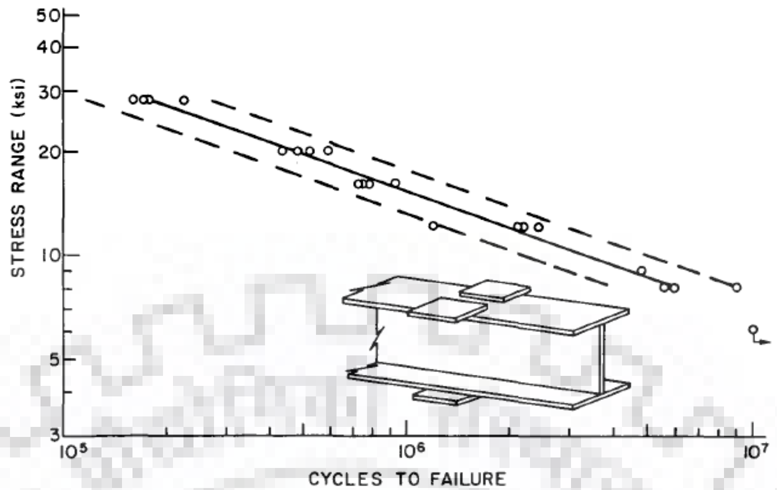

Figure 49 S-N curve for 102 mm attachments welded longitudinally

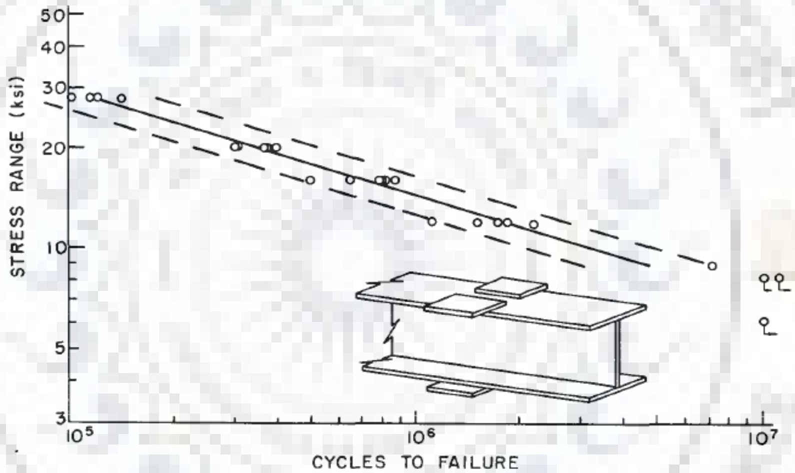

Figure 50 S-N curve for 102 mm attachments welded all around

Data points were collected from Fig. 49 and Fig. 50 and were statistically analyzed using prediction interval and following graph was obtained.

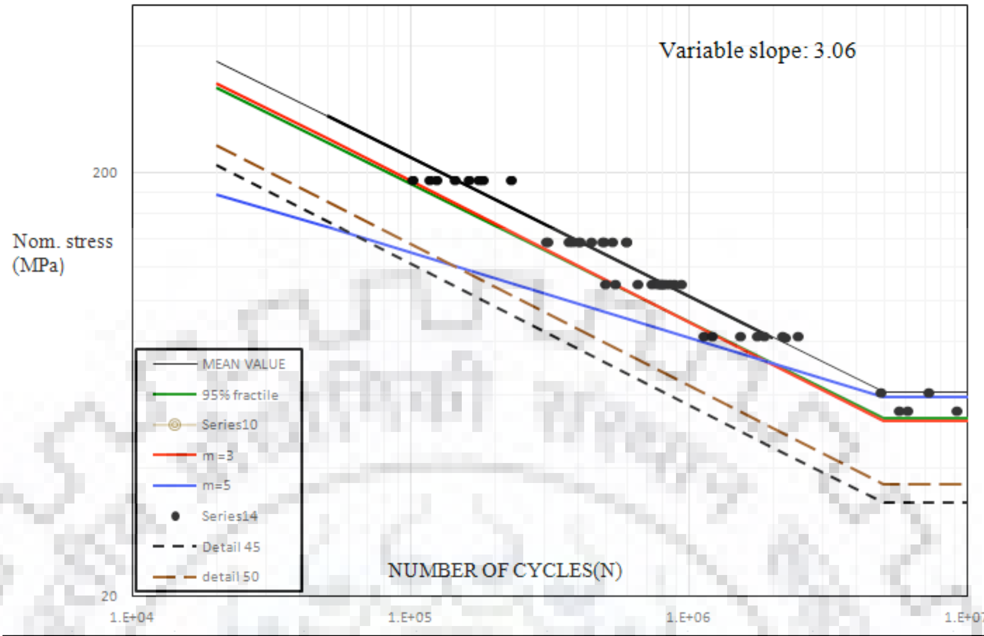

Figure 51. Test results of series 3_4_NLC 24 without run out shown on Logarithmic curve

Fig. 51 shows the statistical result of series 3_4_NLC 24. Statistical analysis gives a value of 71 MPa for 95% fractile and 81 MPa for 50% fractile for a constant slope m=3 calculated at 2 million cycles. Also, 72 MPa for 95% fractile and 82 MPa for 50% fractile for a variable slope m = 3.06 calculated at 2 million cycles.

For series 3_4_NLC 24 we have also done the statistical analysis for the sub series separately and there lies a difference between the two. The statistical results shows that the specimen which are being welded all around possess less fatigue strength than the specimens only welded longitudinally.

Statistical results for specimens **welded all around** gives a value of 67 MPa for 95% fractile and 77 MPa for 50% fractile for a constant slope m=3 calculated at 2 million cycles. Also, 70 MPa for 95% fractile and 79MPa for 50% fractile for a variable slope m = 3.19 calculated at 2 million cycles.

Statistical results for specimens only **welded longitudinally** gives a value of 75 MPa for 95% fractile and 85 MPa for 50% fractile for a constant slope m=3 calculated at 2 million cycles. Also, 70 MPa for 95% fractile and 79 MPa for 50% fractile for a variable slope m = 3.06 calculated at 2 million cycles.

4. Statistical evaluation of series 3-4-NLC 25

Length of the attachment is 204 mm, width of the attachment is 76 mm and thickness of the attachment is 7.2 mm.

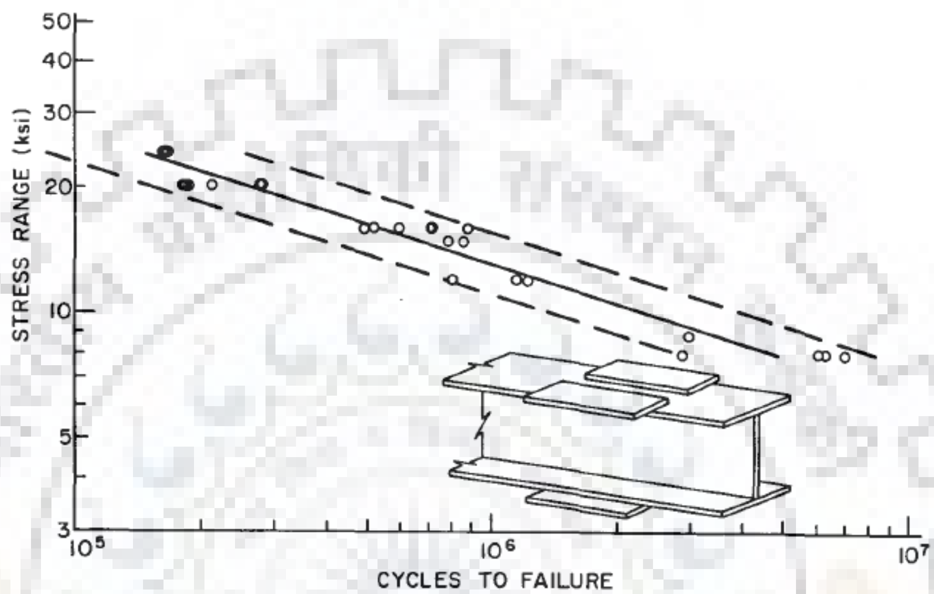

Figure 52. S-N curve for 204 mm attachments

Data points were collected from Fig. 47 and were statistically analyzed using prediction interval and following graph was obtained.

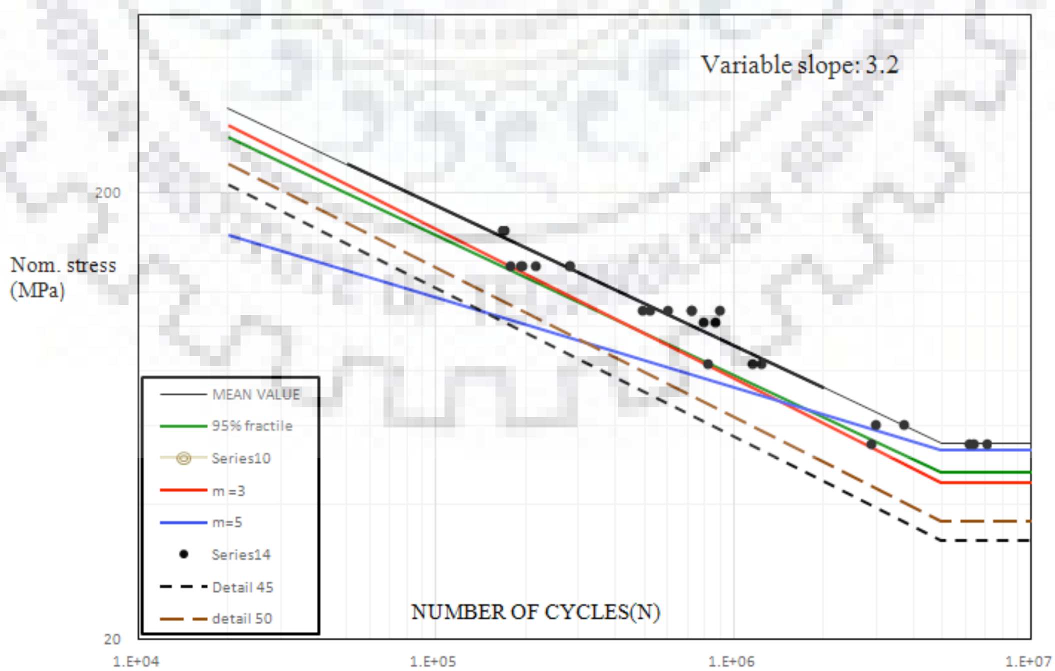

Figure 53. Test results of series 3_4_NLC 25 without run out shown on Logarithmic curve

Fig. 53 shows the statistical result of series 3_4_NLC 25. Statistical analysis gives a value of 61 MPa for 95% fractile and 72 MPa for 50% fractile for a constant slope m=3 calculated at 2 million cycles. Also, 63 MPa for 95% fractile and 73 MPa for 50% fractile for a variable slope m = 3.2 calculated at 2 million cycles.

From the statistical results obtained above we may conclude that the fatigue strength of the specimen decreases as the length of the attachment increases. Specimens with lengths of the attachment 7.1 mm have maximum value of fatigue strength for 95% survival probability at 2 million cycles.

4.4.5 Statistical evaluation of source 27

Total 10 series belongs to source ID number 27. These are 3_5_LCW 11; 3_5_LCW 12; 3_5_LCW 13; 3_5_LCW 14; 3_5_LCW 17; 3_5_LCW 17a; 3_5_LCW 18; 3_5_LCW 19; 3_5_LCW 20; 3_5_LCW 21. Series 3_5_LCW 21 has flanged splice beam which is not a part of our detail. This Series belongs to table 8.3 of Eurocode 3.1-9 either to detail 3 or detail 9.

Also source consists of two types of beams (i) Rolled beams (ii) Welded beams. Statistical analysis of both the beams done separately also thinking there may might lie a difference in the fatigue strength for both types of beams. Specimens for these series are shown in Fig. 54.

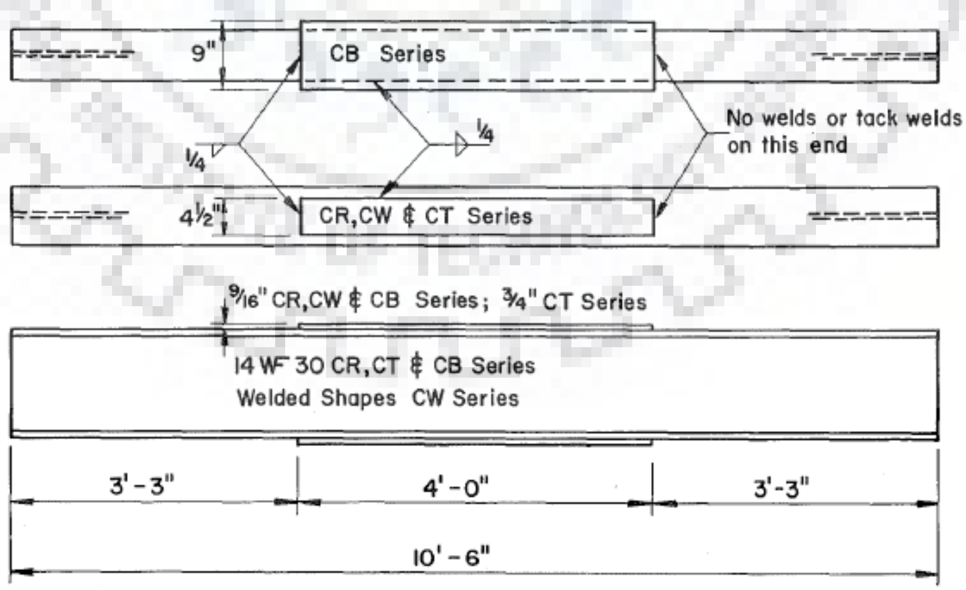

Figure 54. Details of beams with cover plate attached to each flange

In some of the series the ends are welded whereas in some of the series there are unwelded ends. All the test data are given in tabular form. Source quality is good. We were able to get most of the data. Three different steel grades are used. These are A36, A441, A514.

1. **Statistical Evaluation of series 3-5-LCW 11**

The series consist of both welded and rolled beams. Steel grade used is A36. Data points were plotted on S-N curve and following results was obtained. Value of fatigue strength has been calculated for 95% survival probability at 2 million cycles.

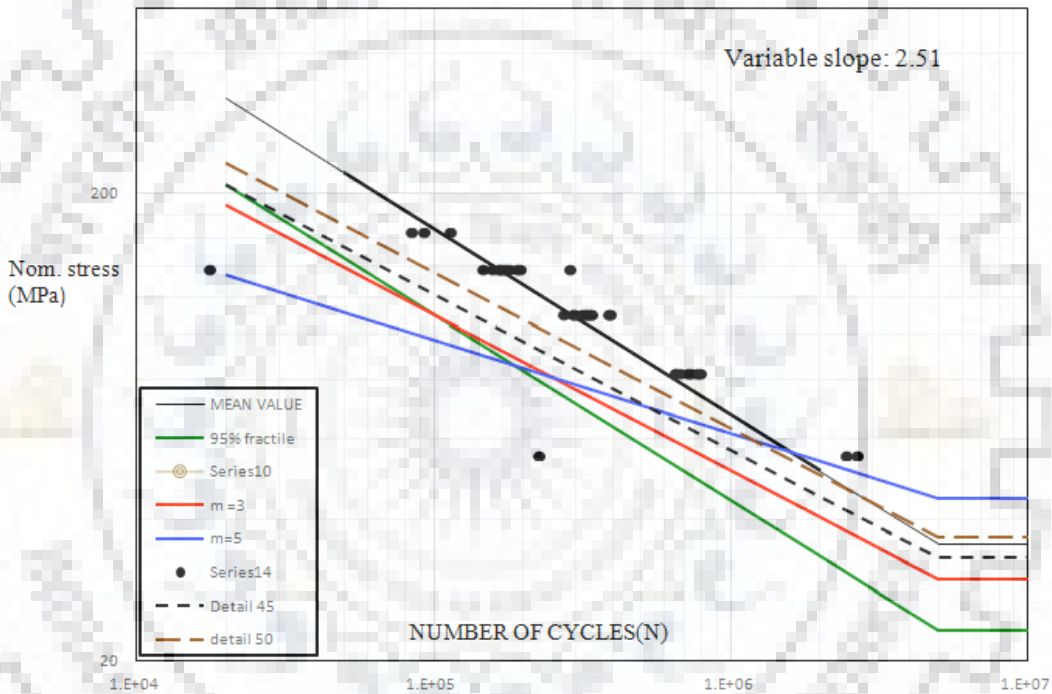

Figure 55. Test results of series 3-5-LCW 11 without run out shown on Logarithmic curve

Fig. 55 shows the statistical result of series 3_5_LCW 11. Statistical analysis gives a value of 41 MPa for 95% fractile and 58 MPa for 50% fractile for a constant slope m=3 calculated at 2 million cycles. Also, 33 MPa for 95% fractile and 51 MPa for 50% fractile for a variable slope m = 2.51 calculated at 2 million cycles.

In Fig. 55 we see there are two data points which seems that they do not belongs to the entire population. So the statistical analysis has been done by removing these 2 points from the test data and following results is obtained. There is an increase in the value from 41 MPa to 55 MPa for 95% survival probability.

2. Statistical Evaluation of series 3-5-LCW 12

The series consist of both welded and rolled beams. Steel grade used is A441. Data points were plotted on S-N curve and following results was obtained. Value of fatigue strength has been calculated for 95% survival probability at 2 million cycles.

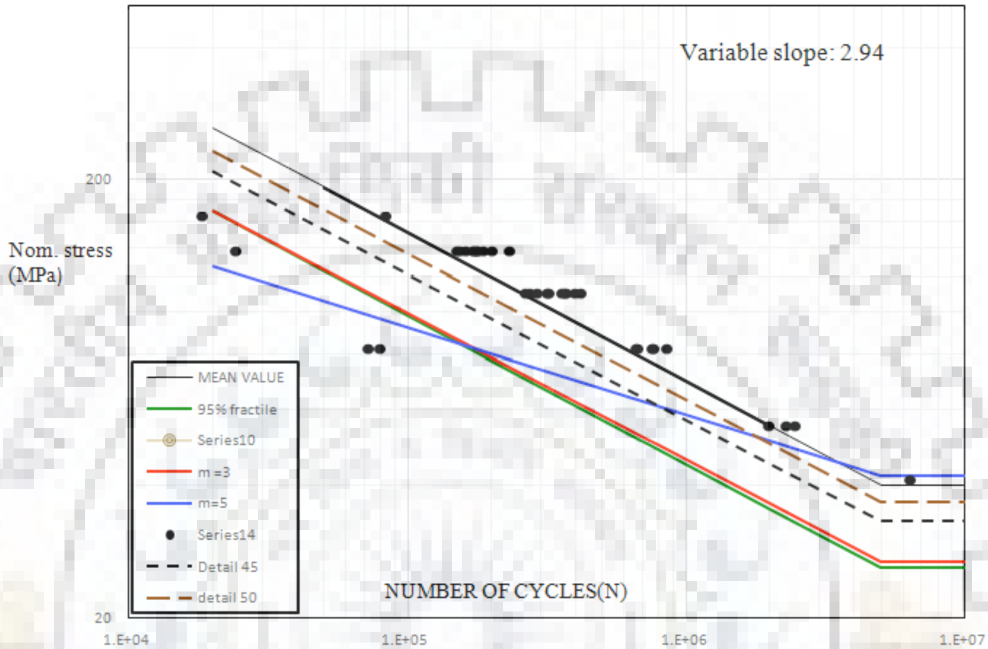

Figure 56. Test results of series 3-5-LCW 12 without run out shown on Logarithmic curve

Fig. 56 shows the statistical result of series 3_5_LCW 12. Statistical analysis gives a value of 37 MPa for 95% fractile and 56 MPa for 50% fractile for a constant slope m=3 calculated at 2 million cycles. Also, 36 MPa for 95% fractile and 55 MPa for 50% fractile for a variable slope m = 2.94 calculated at 2 million cycles.

In Fig. 56 we see there are two data points, which seems that they do not belongs to the entire population. So the statistical analysis has been done again by removing these 2 points from the test data and following results is obtained. There is an increase in the value from 41 MPa to 55 MPa for 95% survival probability.

In the similar ways statistical analysis for all the series was done. Out of 25 series for Detail 6 (Cover plate welded on beam flange) only 10 series shows good statistical results. These are: 3_4_NLC 22; 3_4_NLC 23; 3_4_NLC 24; 3_4_NLC 25, 3_5_LCW 11; 3_5_LCW 12; 3_5_LCW 17; 3_5_LCW 17a; 3_5_LCW 18; 3_5_LCW 19.

Chapter 5 CONCLUSIONS

Statistical analysis for fillet welded lapped joint (detail 5) and cover plates welded on beams flanges (detail 6) following conclusion are made.

1. Out of 27 series available for fillet welded lapped joints (Detail 5) only 6 series gives good statistical results for 95% survival probability at 2 million cycles.
2. The fatigue value for longitudinally welded fillet lapped joint can be increased from recommended 45 MPa to 56 MPa.
3. Also, during the analysis we found that code for transversely welded fillet lapped joint was missing in EC 3.1-9 whereas old data is already available for analysis and also given in IIW codes. From the statistical analysis done for transversely welded fillet lapped joint the value of fatigue strength for the same can be 71 MPa.
4. Out of 25 series available for cover plates welded on beams (detail 6) 10 series gives good statistical results with a higher value of fatigue strength than 50 N/mm^2.
5. In Eurocode 3.1-9 only one attachment on beams are considered while we also have test data available for two attachments welded on each beam flange. So, therefore one more column for 2 attachments welded on beam flange must be added.
6. In some of the data, there are some data points which seem that they does not belong to the entire population, in this we have assumed that may be these specimens show some type of defects during testing so we try to exclude these data points and we have seen that the statistical results were improved i.e. giving higher value of fatigue strength and also the slope of the curve is approximately parallel to the constant slope line i.e. $m=3$.
7. The fatigue strength obtained for one attachment can be increased from recommended 45 MPa to 50 MPa
8. Statistical analysis for plates wider than the beam flange gives poor value of fatigue strength than recommended in EC 3.1-9.
9. No data for hollow beams have been available in the commentary for doing statistical analysis.
10. Also the fatigue strength for two attachments on beam flange can be recommended to be 71 MPa for cover length below 100 mm and 56 MPa for cover plate length above 100 mm as per the statistical results obtained for 95% survival probability at 2 million cycles.

REFERENCES

1. EN 1993-1-9, Eurocode 3: Design of steel structures: Fatigue strength of steel structures, European Committee for standardization, Brussels, 2005.
2. Kim, W. H.; Laird, C. "Crack nucleation and stage I propagation in high strain fatigue—II. Mechanism", Acta Metallurgica, 1978, 26 (5), 789–799.
3. Hirt, M., Bez, R., Nussbaumer, A. Construction Métallique – Notions fondamentales et méthodes de dimensionnement, PPUR Lausanne, TGC 10, 2006.
4. Wöhler A, Versuche uber die festigkeit der eisenbahnwagenachsen, zeitschrift fur bauwesen, vol 10, 1860 (in German), with English summary in engineering, vol 4, 1867, pp. 160-161.
5. Alain Nussbaumer, Fatigue Design of Steel and Composite Structures, 1st ed., Ernst & Sohn Wiley company, Berlin, 2011, pp. 3-13.
6. EN 1090-2, Execution of steel structures and aluminium structures – Part 2: Technical requirements for steel structures, European Committee for Standardization, Brussels, 2008.
7. Schijve J. Fatigue of structures and materials, Kluwer Academic Publ., The Netherlands, 2001 (revised and re-edited in 2009).
8. English CA and Hyde JM, Radiation Embrittlement of Reactor Pressure Vessel Steels, comprehensive structural integrity, Vol. 6, Elsevier Science, pp. 351-398, 2007
9. Bathias C, Paris PC, Gigacycle Fatigue in Mechanical Practice. Publisher: Marcel Dekker. New York, Pp.295, 2005
10. IIW, (2009). International Institute of Welding (IIW): Recommendations for fatigue design of welded joints and components. A. Hobbacher (ed.), Doc. XIII-1965-08, IIW commission XIII
11. ECCS, (1985). Recommendations for the Fatigue Design of Steel Structures, P043 European Convention for Constructional Steelwork, Brussels.
12. AISC, (2005). Steel Construction Manual, Thirteenth Edition, American Institute of Steel Construction (AISC), Chicago, USA
13. Alain Nussbaumer, Fatigue Design of Steel and Composite Structures, 1st ed., Ernst & Sohn Wiley company, Berlin, 2011, pp.163-177.

14. C. R. A. Schneider and S. J. Maddox. Best practice guide on statistical analysis of fatigue data, IIW-Doc. XIII-WG1-114-03, 2003, Pp. 7
15. G. J. Hahn and W. Q. Meeker. *Statistical intervals – A Guide for Practitioners*. Wiley, New York, 1991, Pp. 25,60.
16. N. R. Draper and H. Smith. *Applied regression analysis*. Wiley, 1981, Pp. 21-22.
17. ISO/FDIS 12107. Metallic materials – Fatigue testing – Statistical planning and analysis of data, 2002.
18. G. Sedlaeck, A. Hobbacher, A. Nussbaumer, J. Stotzel, first edition, JRC European Commission, Europe, October 2007, Pp. 21-32
19. Japanese Society of Steel Construction, Fatigue Design recommendations for steel structures, 2nd ed., Japan, 1995.
20. T. R. Gurney and S. J. Maddox, A re-analysis of fatigue data for welded joints in steel, Welding research International,, Vol. 3, 1973.
21. D. S. Macfarlane and J. D. Harrison, Some fatigue tests of load carrying transverse fillet welds, British welding journal, December 1965, Pp. 613-623.
22. D. E. Baxter and G. F. Modlen, Some factors affecting the fatigue strength of the welds, British Welding Journal, April 1966, Pp. 184-188
23. F. E. Brine and H. G. Baron, Effect of sot peening on the fatigue properties of maraging steel and Al-Zn-Mg alloy, British welding journal, November 1968, Pp. 541-543.
24. Manfried A. hirt, La résistance à la fatigue des poutres en âme pleine composéessoudées effet des plaquettes et goussets soudés à l'aile, December 1975.
25. C.G. Schilling, K. H. Klippstein, J. M. Barsom, and G. T. Blake, Fatigue of welded steel bridge member under variable amplitude loadings, NCHRP report 188, Washington D.C. 1978.
26. John W. Fisher, Pedro A. Albrecht, Ben T. Yen, David J. Klingerman, and Bernard M. McNamee, Fatigue strength of the steel beams with welded stiffeners and attachments, Washington, D.C, 1974.
27. John W. Fisher, karl H. Frank, Manfred A. Hirt, and Bernard M. McNamee, Effects of weldment on the fatigue strength of welded beams, Fritz Engineering Laboratory report No. 334.2, September 1969.